การสังเคราะห์ ดัดแปลง และการประยุกต์ใช้ซิลิกานาโนพาทิเคิลในฐานฟันปลอมพอลิเมทิลเมทาคริเลต

นายพรพจน์ เจียงกองโค

วิทยานิพนธ์นี้เป็นส่วนหนึ่งของการศึกษาตามหลักสูตรปริญญาวิทยาศาสตรดุษฎีบัณฑิต
สาขาวิชาทันตกรรมประดิษฐ์ ภาควิชาทันตกรรมประดิษฐ์
คณะทันตแพทยศาสตร์ จุฬาลงกรณ์มหาวิทยาลัย
ปีการศึกษา 2560
ลิขสิทธิ์ของจุฬาลงกรณ์มหาวิทยาลัย

THE SYNTHESIS, MODIFICATION AND APPLICATION OF SILICA NANOPARTICLES

IN POLYMETHYL METHACRYLATE DENTURE BASE

Mr. Pornpot Jiangkongkho

A Dissertation Submitted in Partial Fulfillment of the Requirements

for the Degree of Doctor of Philosophy Program in Prosthodontics

Department of Prosthodontics

Faculty of Dentistry

Chulalongkorn University

Academic Year 2017

Copyright of Chulalongkorn University

Thesis Title THE SYNTHESIS, MODIFICATION AND APPLICATION
OF SILICA NANOPARTICLES IN POLYMETHYL
METHACRYLATE DENTURE BASE
By Mr. Pornpot Jiangkongkho
Field of Study Prosthodontics
Thesis Advisor Associate Professor Mansuang Arksornnukit, Ph.D.

Accepted by the Faculty of Dentistry, Chulalongkorn University in Partial Fulfillment of the Requirements for the Doctoral Degree

---Dean of the Faculty of Dentistry

(Assistant Professor Suchit Poolthong, Ph.D.)

THESIS COMMITTEE

---Chairman

(Assistant Professor Orapin Komin, Ph.D.)

---Thesis Advisor

(Associate Professor Mansuang Arksornnukit, Ph.D.)

---Examiner

(Natthavoot Koottathape, Ph.D.)

---Examiner

(Assistant Professor Wacharasak Tumrasvin, Ph.D.)

---External Examiner

(Associate Professor Thosapol Piyapattamin, Ph.D.)

พรพจน์ เจียงกองโค : การสังเคราะห์ ดัดแปลง และการประยุกต์ใช้ซิลิกานาโนพาทิเคิลใน ฐานฟันปลอมพอลิเมทิลเมทาคริเลต (THE SYNTHESIS, MODIFICATION AND APPLICATION OF SILICA NANOPARTICLES IN POLYMETHYL METHACRYLATE DENTURE BASE) อ.ที่ปรึกษาวิทยานิพนธ์หลัก: รศ. ทพ. ดร. แมนสรวง อักษรนุกิจ, หน้า.

การศึกษานี้มีวัตถุประสงค์เพื่อหาปริมาณการดูดซับทางเคมีของสารคู่ควบ แกมมาเมทาคริ ลอกซีโพรพิลไตรเมทอกซี (เอ็มพีเอส) บนพื้นผิวซิลิกานาโนพาทิเคิล และศึกษาหาปริมาณซิลิกานาโน พาทิเคิล ปริมาณสารคู่ควบเอ็มพีเอสที่ใช้ในการดัดแปลงซิลิกานาโนพาทิเคิล ว่ามีผลต่อค่าความ แข็งแรง โมดูลัส และค่าความแข็งแกร่ง ในวัสดุฐานฟันปลอมที่ผ่านการเสริมแรงด้วยซิลิกานาโนพาทิ เคิลที่ถูกดัดแปลงอย่างไร ปริมาณสารควบคู่เอ็มพีเอสบนพื้นผิวซิลิกานาโนพาทิเคิล จะถูกวัดด้วย กระบวนการวิเคราะห์หาปริมาณธาตุ ตอนแรกแบ่งกลุ่มทดลองเป็น 6 กลุ่ม กลุ่มละ 8 ชิ้นตัวอย่าง โดยใช้ซิลิกานาโนพาทิเคิล ที่ผ่านการดัดแปลงพื้นผิวด้วยสารคู่ควบเอ็มพีเอส จะถูกผสมเข้าไปในโมโน เมอร์ของวัสดุทำฐานฟันปลอมด้วยสัดส่วน 0.25 0.5 1 5 10 และ 15% โดยปริมาตร กลุ่มที่ไม่มีซิลิ กานาโนพาทิเคิลที่ผ่านการดัดแปลง จะเป็นกลุ่มควบคุม ในตอนที่สอง แบ่งกลุ่มทดลองเป็น7กลุ่ม กลุ่มละ 8 ตัวอย่าง โดยแต่ละกลุ่มจะเสริมแรงซิลิกานาโนพาทิเคิลที่ผ่านการดัดแปลงสภาพพื้นผิวด้วย ปริมาณสารคู่ควบที่ต่างกันดังนี้ 0 0.061 0.123 0.246 0.493 0.987 และ 1.974 กรัมเอ็มพีเอสต่อซิ ลิกานาโนพาทิเคิลหนึ่งกรัม นำไปผสมในโมโนเมอร์ของฐานฟันปลอม โมโนเมอร์ในทุกกลุ่มจะถูก นำไปใช้ในการขึ้นรูปฐานฟันปลอม ค่าความแข็งแรงดัดขวาง ค่าโมดูลัส และค่าความแข็งแกร่ง จะถูก ทดสอบด้วยเครื่องทดสอบแบบสากล การวิเคราะห์ผลด้วยความแปรปรวนแบบทางเดียวและการ เปรียบเทียบพหุคูณพบว่า กลุ่มที่ใช้ปริมาณสารคู่ควบเอ็มพีเอส 0.246 กรัมเอ็มพีเอสต่อซิลิกานาโน พาทิเคิลหนึ่งกรัม และปริมาณซิลิการนาโนพาทิเคิล 1 % โดยมวล จะให้ค่าความแข็งแรงดัดขวาง ค่า โมดูลัส และค่าความแข็งแกร่งที่สูงที่สุดอย่างมีนัยสำคัญทางสถิติที่ระดับความเชื่อมั่น 95%

ภาควิชา   ทันตกรรมประดิษฐ์   ลายมือชื่อนิสิต ....

สาขาวิชา   ทันตกรรมประดิษฐ์   ลายมือชื่อ อ.ที่ปรึกษาหลัก ....

ปีการศึกษา 2560

5576055032 : MAJOR PROSTHODONTICS

KEYWORDS: FLEXURAL PROPERTIES / MODIFICATION / NANOSILICA / SILANE COUPLING AGENT / SYNTHESIS

PORNPOT JIANGKONGKHO: THE SYNTHESIS, MODIFICATION AND APPLICATION OF SILICA NANOPARTICLES IN POLYMETHYL METHACRYLATE DENTURE BASE. ADVISOR: ASSOC. PROF. MANSUANG ARKSORNNUKIT, Ph.D., pp.

This study aimed to investigate amount of **γ**-methacryloxypropyltrimethoxysilane (MPS) silanized on experimental nanosilica particles (NPs), amount of NPs and amount of MPS silanized NP on flexural strength (FS), flexural modulus (FM), and fracture toughness (FT) of NP reinforced polymethymethacrylate (PMMA). The chemisorbed amount of MPS was determined using elemental analysis. Six groups (n=8) were prepared with chemisorbed amount and mixed with PMMA-monomer to make 0.25, 0.5, 1, 5, 10 and 15% (w/w) of NP reinforced PMMA. PMMA without NP served as control. Seven groups (n=8) were prepared with 1% of NPs silanized with 0, 0.061, 0.123, 0.246, 0.493, 0.987, and 1.974 g_{MPS}/g_{silica} and mixed with PMMA-monomer to make NPs reinforced PMMA. FS, FM, and FT were determined using 3-point bending test. One-way ANOVA and multiple comparisons showed that 0.246 g_{MPS}/g_{silica} of 1% amount of silanized NP group was significantly highest in FS, FM, and FT compared to the others (p<0.05).

Department:	Prosthodontics	Student's Signature ....
Field of Study:	Prosthodontics	Advisor's Signature ....
Academic Year:	2017	

ACKNOWLEDGEMENTS

จุฬาลงกรณ์มหาวิทยาลัย

CHULALONGKORN UNIVERSITY

CONTENTS

จุฬาลงกรณ์มหาวิทยาลัย
CHULALONGKORN UNIVERSITY

INTRODUCTION

Nanotechnology is the understanding and control of matter at the dimension between 1 to 100 nanometers. Nanoparticles have a very high surface area to volume ratio, resulting in an increase of molecular interaction between polymer and nanoparticles in composite nanomaterial[1]. At nanoscale, the inorganic nanoparticles are used to reinforce the polymer matrix. However, it should be pointed out that the effect of nanoparticle enhancement depends on the size of the particles and the level of their dispersion[2].

Nanosilica are frequently used as fillers to improve the properties of the material such as abrasion resistance, mechanical properties, and refractive index. For optical transparency and optimal performance, the small size and a homogeneous distribution of these nanoparticles in the matrix are essential[3]. The Stöber method was firstly introduced using ammonia catalyzed hydrolysis and condensation in low molecular-weight of alcohol as solvent to produce uniform nanosilica[4]. The size and dispersion of nanosilica are controlled by the concentration of tetraethyorthosilicate, water, and ammonia[5-8]. However, inorganic particles cannot be dispersed in nonpolar organic polymer, unless a dispersing agent is used. For this purpose, silane coupling agents are oftenly used as a dispersing agent to form stable chemical bonds between inorganic particles and organic polymer materials. Moreover, silane could improve the dispersive stability of the particles in a polymer and enhance the mechanical

properties of polymer based composite materials[9]. The high viscosity of organic polymer made it difficult to disperse nanoparticles into the polymer matrix. The difficulty in dispersion limits the effect of nanoparticles to improve mechanical properties of polymer. In order to solve this problem, predispersion of the nanoparticles in the monomer or pre- polymer before preparation of the nanocomposites is recommended[2].

γ- methacryloxypropyltrimethoxysilane (MPS) is a dominant silane coupling agent used in dentistry to modify the surface of silica[9]. An important factor is the amount of MPS covering the surface of the nanosilica. Theoretically, calculations yield two estimated amount of MPS, depending on the orientation of the MPS molecules[10]. If the MPS molecule orients perpendicular to the surface, it is estimated that 6.9 μmol of MPS needed to create a monolayer covering 1.0 m^2 of nanosilica surface. If the MPS molecule orients parallel to the surface, which included hydrogen bonding between the carbonyl group in MPS and a hydroxyl group of the oxide apart from siloxane bond, only 3.0 μmol of MPS is needed for a monolayer covering 1.0 m^2 of silica surface[10]. The calculations of the aforemention above based on the computer simulation. While, amount of MPS for monolayer coverage on silica surface calculation was 12.82 μmol/m^{2} [11]. Posthumus *et al*[12] have reported that the actual values can be deviated from both Arkles's equation and their calculation due to the incomplete coverage; the increase in molecular weight of MPS due to homocondensation. Therefore, the homocondensed molecule is too large to react on the silica surface, resulting in the

multilayers formation. Söderholm and Shang[13] suggested that an amount of MPS for monolayer coverage on silica surface was from 1.59 µmol/m^2. This amount was approximately 8 times lower than computation from Akle's equation (12.82 µmol/m^2). The actual amounts of MPS used were lower than the amount needed for a complete monolayer coverage[12, 13], based on both computer simulation and Akles's equation. Quantitative information on the silanizaton of MPS on nanosilica is still inconclusive.

Polymethymethacrylate (PMMA) is a commonly used material to fabricate denture base since the 1940s[14]. It has the advantages of low cost, simple fabrication process, light weight, satisfactory aesthetics, color matching ability, and easy to finishing and polishing[15]. However, some disadvantages still remain which include low strength and toughness. Many studies have been carried out to improve the mechanical properties of the denture base materials by adding fillers into PMMA denture base[16, 17]. It was reported that monolayer chemisorbed of MPS on alumina was adequate for improving the mechanical properties of PMMA denture base[17]. However, there are no studies concerning the amount of MPS on nanosilica on the mechanical properties of the nanosilica reinforced PMMA. In this study, predispersion of monolayer chemisorbed of silanized nanosilica in liquid monomer of PMMA was used to obtain a homogenous suspension, which was subsequently mixed with polymer powder of PMMA. It was hypothesized that this process could provide homogenous material which improved the mechanical properties of PMMA denture base.

Therefore, the objectives of this study were to investigate the chemisorbed amounts of silanized on experimental nanosilica and to investigate the effect of various amount of experimental nanosilica and various amount of MPS silanized on the experimental nanosilica on mechanical properties of experimental nanosilica reinforced PMMA denture base. The null hypotheses were that there would be no differences in the mechanical properties of PMMA denture base reinforced with various amount of experimental nanosilica and amount of silanized on the experimental nanosilica.

REVIEW LITERATURE

Nanomaterial[18]

Nanomaterial reinforcements for polymer composites have in recent years been the subject of intense research and development. Nanomaterial is materials having at least one dimension below about 100 nm. The small size offers some level of controllable performance that is different from the expectations developed in the macroscale. The advantages that have been cited to date are that nanocomposites offer improved properties at significantly lower filler loading levels than would be the case with conventional filler materials. The addition of nanomaterials to polymers is making composite materials significantly impacts mechanical and barrier properties, flame retardancy, and electrical conductivity.

Particle Aggregation and Agglomeration[19]

Aggregates are particles combined by covalent bonds. Agglomerates are particles held together by van der Waals attractive force. Van der waals attractive force is inter-molecular attractive force which comprise of dispersive and dipole-dipole force. Small particles tend to agglomerate. This is due to inter-molecular attractive forces. As the particle sizes decrease, the surface area becomes large relative to mass. The large surface area favors agglomeration. This tendency is much greater for polar particles such as oxides (SiO_2, TiO_2, etc.) than for nonpolar particles such as carbon black. Because polar particles have dipole-dipole forces that greater than dispersive force from nonpolar particle.

Particle Dispersion [19)]

When these particles are charged, they repel each other; uncharged particles are agglomeration as shown in Figure 1. To keep each particle, separate and prevent particles from gathering into larger agglomerates, the attractive forces between individual particles must be reduced. When colloid particle sizes are very small, the surface forces at the interface of particles are large. One of the major surface effects is electrokinetic. When particles hold the same electrical charge (positive or negative), they produce a force of mutual electrostatic repulsion between adjacent particles. When the degree of charge is high, the particles will remain separate, diffuse, and in suspension, as shown in Figure 1a. When the degree of charge is low, it will create the opposite effect. This results in agglomeration as shown in Figure 1b. Charge can be modified and controlled by changing the liquid's pH or changing the ionic species in solution.

(a) Charged Particles   (b) Uncharged Particles
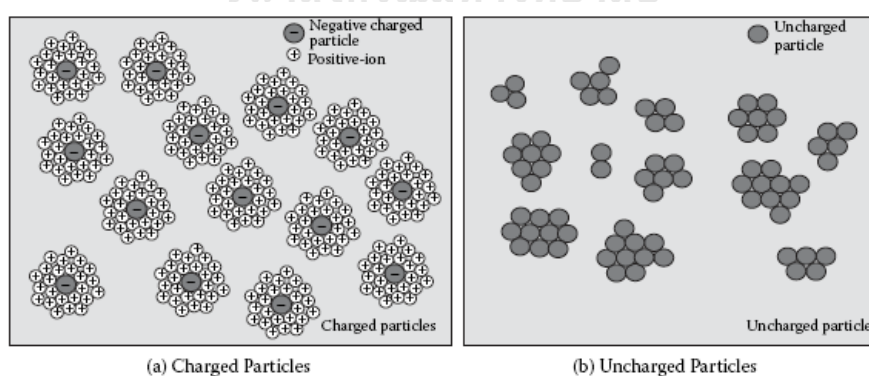
Fig 1. Effect of surface charge on agglomeration.

Electrokinetic Potential and Electrical Repulsion[2, 19, 20)]

The development of a net charge at the particle surface affects the distribution of ions in the surrounding interfacial region, resulting in an increased concentration of counter ions close to the surface. Thus, an electrical double layer exists around each particle (Fig 2). The liquid layer surrounding the particle exists as two parts; an inner region, called the Stern layer, where the ions are strongly bound and an outer, diffuse layer, region where they are less firmly attached. Within the diffuse layer there is a notional boundary inside which the ions and particles form a stable entity. When a particle moves, ions within the boundary move with it, but any ions beyond the boundary do not travel with the particle. This boundary is called the surface of slipping plane. The potential that exists at this boundary is known as the Zeta potential.
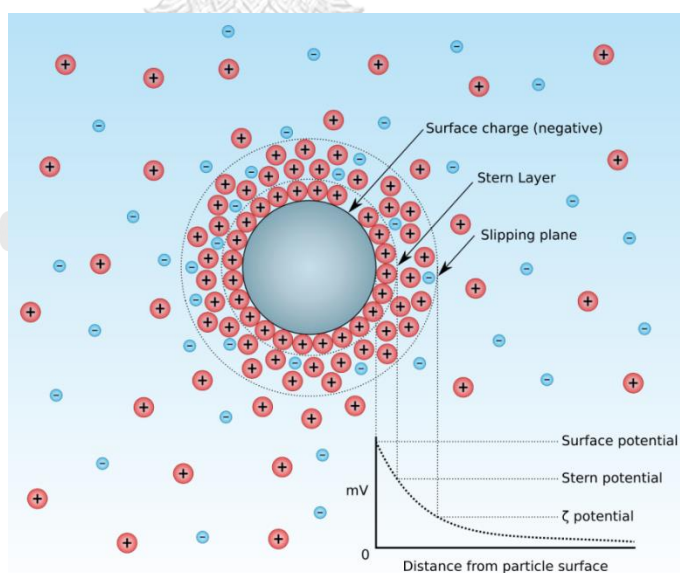
Fig 2. The electrical double layer (stern and diffuse layer), surface potential, zeta potential.

The magnitude of the zeta potential gives an indication of the potential stability of the colloidal system. If all the particles in suspension have a large negative or positive zeta potential then they will tend to repel each other and there is no tendency to agglomerate. However, if the particles have low zeta potential values then there is no force to prevent the particles coming together and agglomerate. The general dividing line between stable and unstable suspensions is generally taken at either +30mV or -30mV. Particles with zeta potentials more positive than +30mV or more negative than -30mV are normally considered stable (Fig 3).
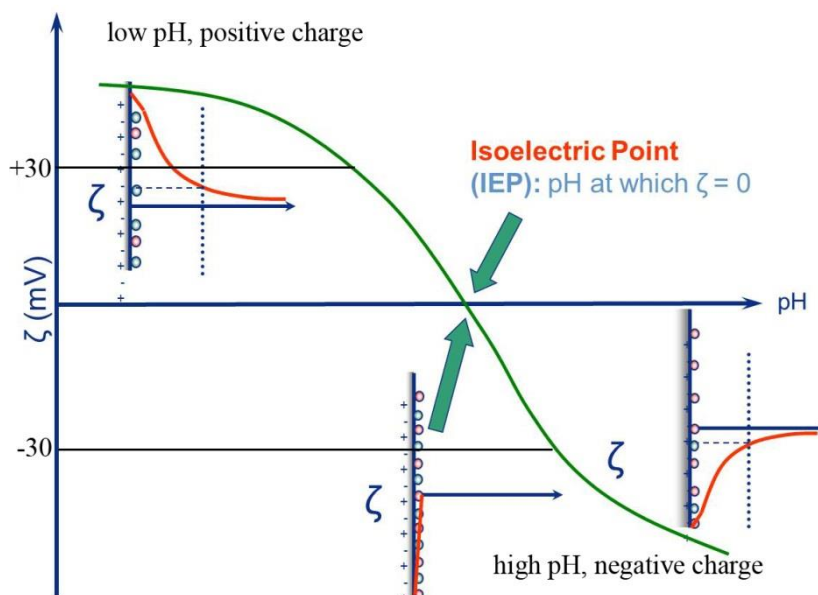
Fig 3. Zeta potential at different pH, isoelectric point (IEP) pH at 0 potential.

Attractive Inter-Particle Forces[19)]

Nonpolar particles such as carbon black have dispersive forces. This causes them to agglomerate. Polar particles such as calcium carbonate, silica, titanium dioxide,

and zinc oxide have dipole-dipole attractive forces, which are much stronger and more

difficult to disperse agglomerates (Fig 4).
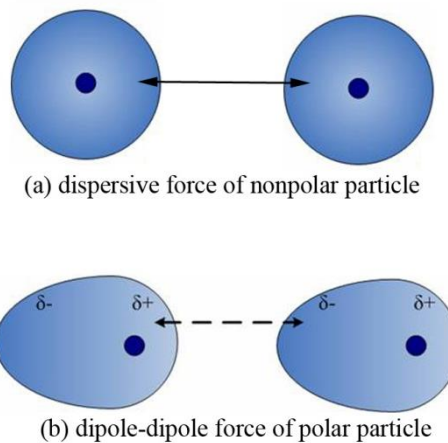
Fig 4. Attractive inter-particle force (a) dispersive force, (b) dipole-dipole force

Silica[21, 22]

The structure of silica (SiO_2) involves each silicon atom having four somewhat

polar covalent bonds with oxygen as shown in Figure 5. SiO_2 exists in crystalline and

amorphous forms.
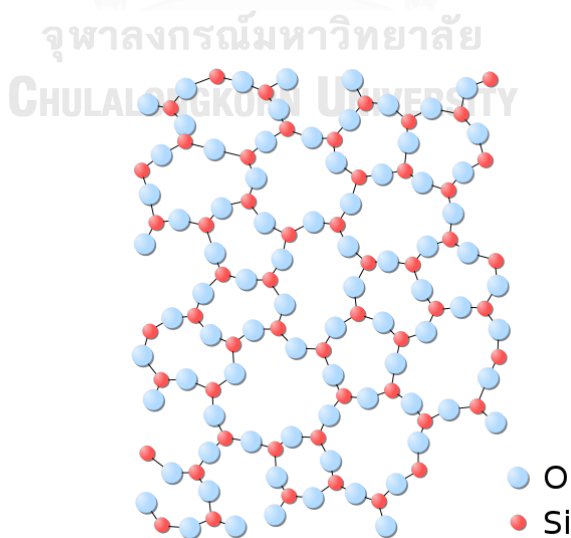
Fig 5. Structure of silica.

The commercial silica used in thermosets and elastomers is amorphous. It has the form of aggregates of primary particles as shown in Figure 6. Synthetic silicas are manufactured by various methods: fumed, electric arc, fused, gel, and precipitated. All synthetic silicas are amorphous in nature, have a chemical composition of SiO_2, and are colorless, odorless, tasteless, fine-particle, white powders.
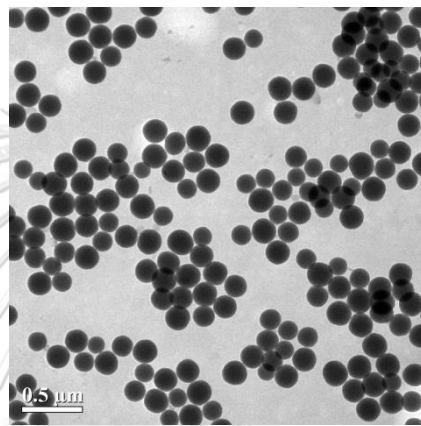
Fig 6. Aggregation of silica

Synthetic silicas are considered polymers of monosilicic acid ($Si(OH)_4$). Iler has developed a model of polymerization starting from monomer $Si(OH)_4$ to form silica. This is shown in Figure 7. In basic solution (B), particles in solution grow in size but decrease in number. In acid solution or in the presence of flocculating salts (A), particles aggregate into three dimensional networks and form gels. [12] Typical primary particle sizes of synthetic silicas are 0.01 to 0.10 μm and a BET surface area of 50 to 800 m^2/g. The refractive index of synthetic silica is 1.45, which is close to the refractive indices of polymers, making it possible to produce translucent and transparent filled

polymer compounds. The surface of synthetic silica contains hydroxyl groups called silanol groups, which easily tend to form hydrogen bonds with water molecules and demonstrate hydrophilic character.
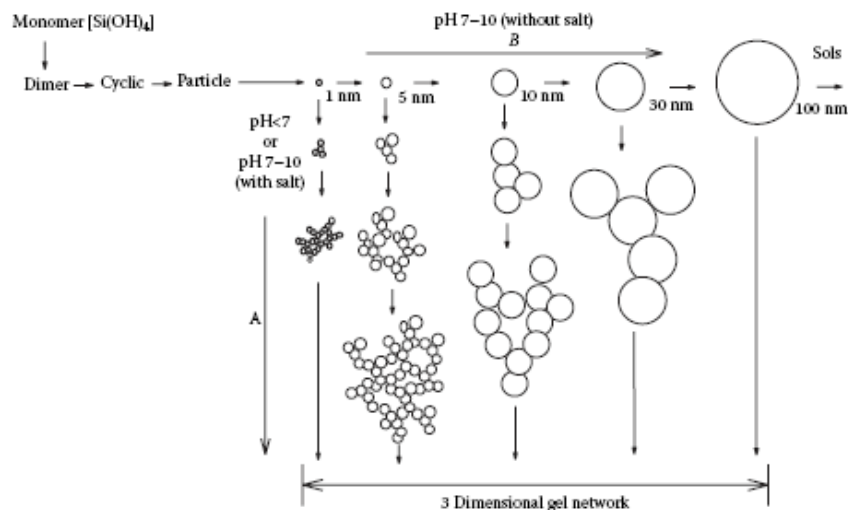

Fig 7. Synthesis of SiO_2 using polymerization of $Si(OH)_4$.

Among the synthetic silica, fumed silica is the most expensive and also has special industrial applications. Fumed silica is prepared by the hydrolysis of silicon tetrachloride vapor above 1000° C. The primary particles of fumed silicas are connected by several other primary particles to show a chain-like aggregate structure. The primary particles of aerogel silica form a large sponge-like mass that is supposedly responsible for the very high internal surface area and microporosity in silica gels.

Sol-gel syntheses of silica are based on the hydrolysis of tetraalkoxysilanes, $Si(OR)_4$, according to the following equation, e.g.:

$$Si(OC_2H_5)+4H_2O \longrightarrow SiO_2+4C_2H_5OH$$
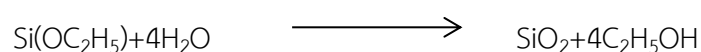
Gelation of silicon alkoxide solutions takes place as a result of the hydrolysis of the silicone alkoxides $Si(OR)_4$ and subsequent polycondensation leading to the formation of polymers and particles with siloxane bonds. The reaction can be expressed by the following formulae:
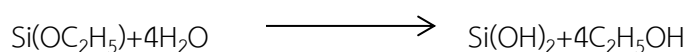
$$Si(OC_2H_5)+4H_2O \longrightarrow Si(OH)_2+4C_2H_5OH$$

$$Si(OH)_4 \longrightarrow SiO_2+H_2O$$

Figure 8 presents the various silica particles as normal, condensed, and water molecule emulsified forms. Normal silica particles are agglomerated with hydrogen bond/dipole-dipole force (Figure 8, top). Under hot storage or shipping conditions, the nano-sized silica particles are chemically aggregated easily due to a self-condensation reaction. Once they are chemically bonded to each other, it is difficult to break down during processing (Figure 8, middle). In the present of water, the polar or hydrogen bond silica agglomerates disperse easily via the presence of large amounts of polar water molecules, because hydrogen bonding is about five times stronger than dipole-dipole force. A large amount of water molecules loosens the agglomeration force between silica particles (Figure 8, bottom). This facilitates dispersion of the silica particles in a polymer matrix.
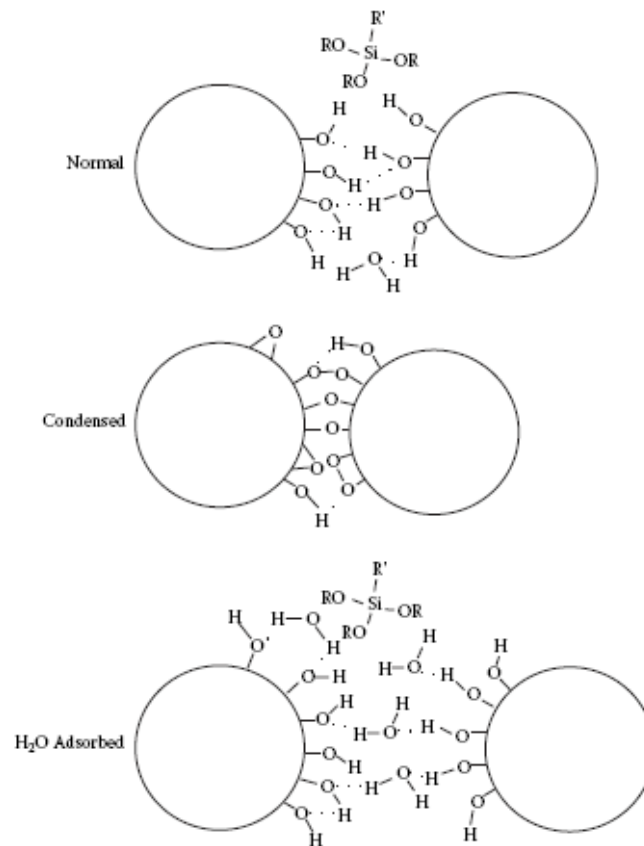
Fig 8. Schematic presents the various silica particles as normal, condensed, and water adsorbed.

Silica primary particles exist in aggregate form (secondary particle structure), similar to carbon black. The aggregate size ranges from a few to a hundred primary particles. The agglomerate form (ternary structures) is formed when the secondary particle further agglomerates during the manufacturing process. Thus, silica particle size structures exist at three levels: (1) primary particles (ultimate particles), (2) secondary particle (aggregates of primary particles), and (3) tertiary particles

(agglomerates of secondary particle). Agglomerates are broken down under the application of high shear stress.

Silica agglomeration and dispersion [22]

It has been found that very small polar particles are difficult to disperse through processing equipment. Strong polar particles are more difficult to disperse than nonpolar particles due to increased dipole-dipole forces. Silica particles tend to easily agglomerate and re-agglomerate, even after mixing. Silica particles are a polar mineral due to the differences in electronegativity between the silicon (1.90) and oxygen (3.44) atoms, while carbon blacks are nonpolar due to the same electronegativity between carbon atoms (2.55). The silica particle in suspension is negatively charged at a certain pH level because of the loss of protons form H_3O^+ molecules located in the spaces between the oxygen atoms of the SiO_2 structure.

Silane hydrolysis and condensation with silica surface [22-24]

The silica particle size decreases to nanometer dimensions, its surface area per unit volume increases. This results in an increase of the dipole-dipole force and the accumulated hydrogen-bonding force between silica particles. To disperse agglomerated silica particles, the inter-particle forces should be reduced by coating the particle surfaces with additives that make the surfaces more compatible with the surrounding polymer. The surface of silica can be modified with surfactant chemicals such as the silanes in Table 1. Silanes help silica dispersion in two ways. First, the chemical coupling of a silane on the silica surface changes the hydrophilic silica surface

to a hydrophobic surface, which makes the surfactant-treated silica surface compatible with hydrophobic polymer chains. The silane-bonded silica surface has improved compatibility with polymer chains. It will be easy to peel off silica particles from the surface of silica aggregates during mixing. Second, the coupling of silane on silica surface reduces the number of hydroxyl groups on the silica surface per unit volume, which implies the reduction of the hydrogen bonding forces and the polarity of between silica surface particles. Thus, the coupling of silane on the silica surface improves silica particle dispersion.

Table1. Type of silane

Functional group	Chemical name	Structural formula
Methacryloxy	3-methacryloxypropyltrimethoxysilane	$(CH_3O)_3SiC_3H_6OCC=CH_2$ with CH_3 and $\overset{\|}{O}$
	3-methacryloxypropylmethyldimethoxysilane	$(CH_3O)_2SiC_3H_6OCC=CH_2$ with CH_3 CH_3 and $\overset{\|}{O}$
Amino	3-aminopropyltrimethoxysilane	$(C_2H_5O)_3SiC_3H_6NH_2$
	3-aminopropyltriethoxysilane	$(CH_3O)_3SiC_3H_6NH_2$

Effect of silane type on silica agglomerate size reduction[22, 23]

The choice of silane should involve matching chemical reactivity, solubility characteristics, structural characteristics and the thermal stability of the silane with the same parameters in the polymer structure.

There are many types of silane which based on the polymer chain. The polymer chain of silane affects silica agglomeration. First, when small-chain silane bonded to the silica surface, it formed a brush-like shape, as illustrated in Figure 9a. The probability of short-chain silane bonding on a silica surface is higher than that of long-chain silane. The trend was that as the chain length of the coupling agents decreased, the agglomerate size also decreased. This appears to be related to the steric hindrance of the long-chain silane and a polarity reduction on the silica surface. When a long aliphatic chain silane bonded on the silica surface, it causes steric hindrance to the next chain approaching to the silica surface as shown in Figure 9b. Second, low-molecular-weight silanes have more functional groups per unit weight to chemically react with silica surface, thus reducing particle interaction between silica particles.
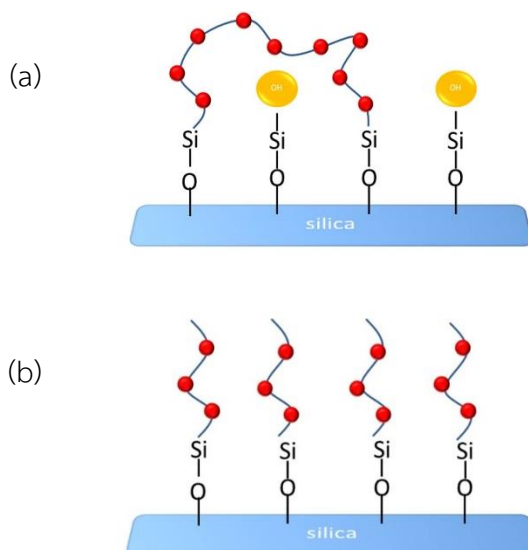
Fig 9. Schematic presentation of different chain length silanes bond on silica (a) short chain, (b) long chain

3-methacryloxypropyltrimethoxysilane (MPS)[9, 13, 23, 25]

The silane most commonly applied in dental composites resin is 3-methacryloxypropyltrimethoxysilane (MPS) (Fig 10), a bifunctional molecule consists of methacrylate and silanol groups capable of forming carbon–carbon and siloxane chains by polyaddition and hydrolytic polycondensation, respectively. The short chain and low molecular weight of MPS provides appropriate bonding between silica nanoparticle and polymer matrix.
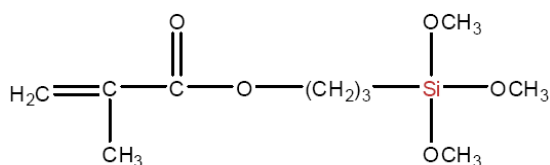
Fig 10. molecular structure of MPS

Calculation amount of silane[9, 12]

Theoretical calculations are two estimates depending on the orientation of the MPS molecules. The molecule is considered as a rod with an orientation perpendicular to the surface. It is estimated that 6.9 μmol/m^2 MPS is needed for a monolayer. In the other hand, the MPS is oriented parallel to the surface, which might be induced by hydrogen bonding between the MPS-carbonyl and a hydroxyl group of the oxide. It estimates only 3.0 μmol/m^2 is needed for a monolayer. However, these estimates are based on one completely filled monolayer. The real values can deviate from these estimates due to incomplete coverage or as a result of the formation of multilayers. When silane used as a coupling agent between silica nanoparticle and polymer matrix, the required amount of silane can be calculated by the following:

$$m_{silane} \text{ (g)} = m_{silica} \text{ (g)} \times M_{silane} \text{ (μmol/m}^2\text{)} \times MW_{silane} \text{ (g/mol)} \times A_{silica} \text{ (m}^2\text{/g)}$$

m_{silane} = amount of silane (g)

m_{silica} = amount of silica (g)

M_{silane} = minimum required for completely covered on silica surface (μmol/m^2)

MW_{silane} = molecular weight of silane (g/mol)

A_{silica} = specific surface area of silica (m^2/g)

Characterization of modification and dispersion

Transmission electron micrograph[26, 27)

Direct imaging of individual nanoparticles is only possible using transmission electron micrograph (TEM). Transmission electron micrograph can provide a real space image on distribution of the nanoparticle and its surface. TEM provides not only atomic resolution lattice images, but also chemical information at a spatial resolution of 1 nm or better, allowing direct identification of the chemistry of a single nanoparticle. With a finely focused electron probe, the structural characteristics of a single nanoparticle can be fully characterized.

Dynamic light scattering (DLS)[28)

This method, also known as photon correlation spectroscopy is primarily used to measure nanoparticulate colloid systems such as emulsions, micelles, liposomes and nanosuspensions. When a laser beam is passed through liquid suspensions containing particles in Brownian motion, it experiences fluctuations in its intensity due to light scattering. In the DLS instrument, measurements of this fluctuation of intensity at a given scatter angle are used to infer the particle size of the suspended particles. The DLS instruments measure the fluctuations in the intensity of the scattered light with time to generate an exponentially decaying autocorrelation function. This function is then analyzed for characteristic decay times, to determine the diffusion coefficient unique to the scattering suspensions and, in conjunction with the Stokes-Einstein equation, the hydrodynamic radius.

$$D = \frac{kT}{6\eta\pi r}$$

D=diffusion constant

K=Bolzmann's constant

T=absolute constant

r=radius of particle

η=viscosity

Specific surface area[29, 30]

Specific surface area aBET is defined as the ratio A/ms (unit: m^2/g) between the absolute surface area and its mass ms (sample weight). The surface area includes all parts of accessible inner surfaces (mainly pore wall surfaces). Precise measurement of the specific surface area of solids uses gas adsorption (nitrogen, krypton) according to Brunauer, Emmett und Teller (BET method). The BET method involves the determination of the amount of the adsorbate or adsorptive gas required to cover the external and the accessible internal pore surfaces of a solid with a complete monolayer of adsorbate. This monolayer capacity can be calculated from the adsorption isotherm by means of the BET equation.

The gases used as adsorptive have to be only physically adsorbed by weak bonds at the surface of the solid (van der-Waals forces) and can be desorbed by a

decrease of pressure at the same temperature. The most common gas is nitrogen at its boiling temperature (77.3 K). In the case of a very small surface area (below 1 m^2/g), the sensitivity of the instruments using nitrogen is insufficient and krypton at 77.3 K should be used.

In order to determine the adsorption isotherm volumetrically, known amounts of adsorptive are admitted stepwise into the sample cell containing the sample previously dried and outgassed by heating under vacuum. The amount of gas adsorbed is the difference of gas admitted and the amount of gas filling the dead volume (free space in the sample cell including connections). The adsorption isotherm is the plot of the amount gas adsorbed (in mmol/g) as a function of the relative pressure p/p_0.

For the multipoint determination, a BET diagram is plotted with

$$y_{BET} = \frac{p/p_0}{n_a(1-p/p_0)} = \frac{C_{BET}-1}{n_{mono} \cdot C_{BET}} \cdot (p/p_0) + \frac{1}{n_{mono} \cdot C_{BET}} = f(x) = i + kx$$

as ordinate against $x = p/p_0$ as abscissa. The plot should give a straight line

$y_{BET} = i + kx$ within the so-called BET relative pressure range (Fig 11). Both the intercept a and the slope b, which are determined by means of linear regression, must be positive. From these values, the monolayer capacity n_{mono} (in mmol/g) can be calculated according to $n_{mono} = 1/(i+k)$. The specific surface area aBET is calculated from the monolayer capacity by assessing a value σ for the average area occupied by each molecule in the complete monolayer:

aBET=n$_{mono}$.σ.N$_A$
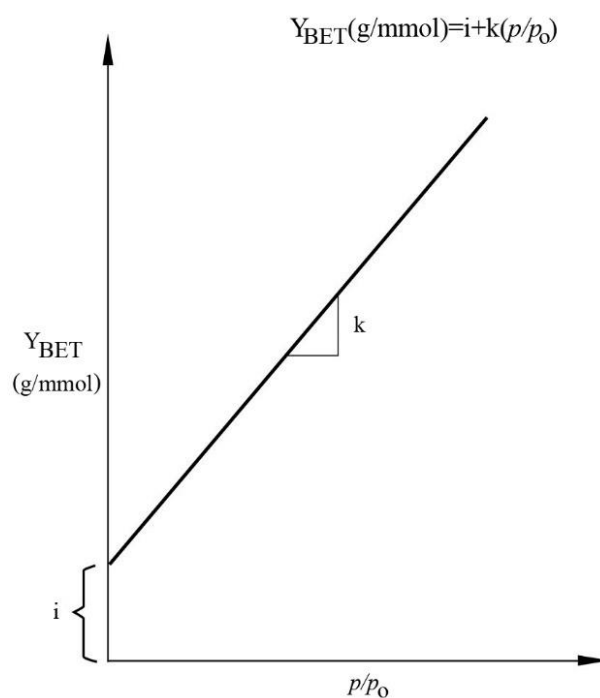
NA is the Avogadro constant.

Fig 11. The plot of straight line yBET $= i + k\, p/p_0$

Molecular cross sectional area values σ for nitrogen and krypton are recommended by the standard ISO 9277:2010 and the IUPAC Recommendations of 1984 as σ = 0.162 nm^2 for nitrogen and σ = 0.202 nm^2 for krypton respectively.

Fourier transform infrared (FTIR)[31]

FTIR is the preferred method of infrared spectroscopy. In infrared spectroscopy, IR radiation is passed through a sample. Some of the infrared radiation is absorbed by the sample and some of it is passed through. The resulting spectrum represents the

molecular absorption and transmission, creating a molecular fingerprint of the sample

(Fig 12). Many substances can be characterized, identified and also quantified.
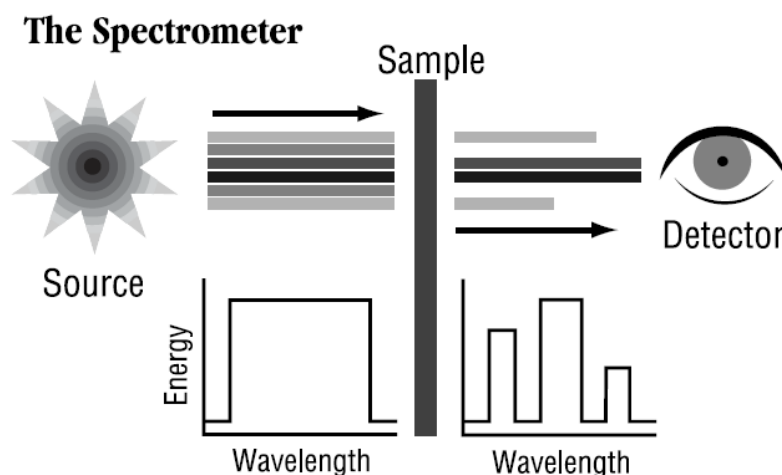

Fig 12. Fourier transform infrared

Zeta potential[20, 32]

The magnitude of the zeta potential gives an indication of the potential stability

of the colloidal system. If all the particles in suspension have a large negative or

positive zeta potential, then they will tend to repel each other and there is no

tendency to agglomeration. However, if the particles have low zeta potential values

then there is no force to prevent the particles coming together and agglomeration.

The general dividing line between stable and unstable suspensions is generally taken

at either +30mV or -30mV. Particles with zeta potentials more positive than +30mV or

more negative than -30mV are normally considered stable.

The most important factor that affects zeta potential is pH. Imagine a particle

in suspension with a negative zeta potential. If more alkali is added to this suspension,

then the particles will tend to acquire a more negative charge. If acid is then added to this suspension a point will be reached where the negative charge is neutralized. Any further addition of acid can cause a buildup of positive charge. Therefore, a zeta potential versus pH curve will be positive at low pH and lower or negative at high pH. The point where the plot passes through zero zeta potential is called the Isoelectric point and is very important from a practical consideration. It is normally the point where the colloidal system is least stable. A typical plot of zeta potential versus pH is shown in figure 13.
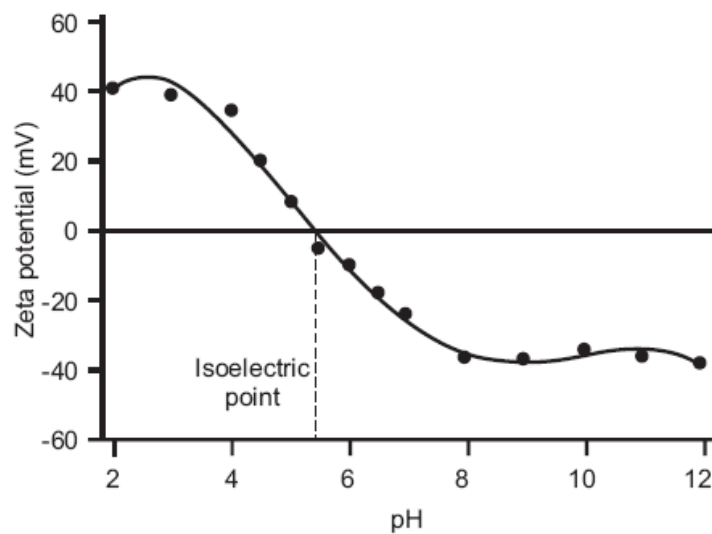
Fig 13. A typical plot of zeta potential versus pH

When an electric field is applied across an electrolyte, charged particles suspended in the electrolyte are attracted towards the electrode of opposite charge (Fig 14). Viscous forces acting on the particles tend to oppose this movement. When

equilibrium is reached between these two opposing forces, the particles move with

constant velocity. The velocity of the particle is dependent on the following factors:

Strength of electric field or voltage gradient.

The Dielectric constant of the medium.

The Viscosity of the medium.

The Zeta potential.

The velocity of a particle in an electric field is commonly referred to as its

Electrophoretic mobility. With this knowledge, we can obtain the zeta potential of the

particle by application of the Henry equation. The Henry equation is:

$$U_E = \frac{2z\varepsilon f(ka)}{3\eta}$$

*Z =*Zeta potential.

U_E=Electrophoretic mobility.

ε=Dielectric constant.

η=Viscosity.

f(Ka)=Henry's function.

Two values are generally used as approximations for the *f(Ka)* determination
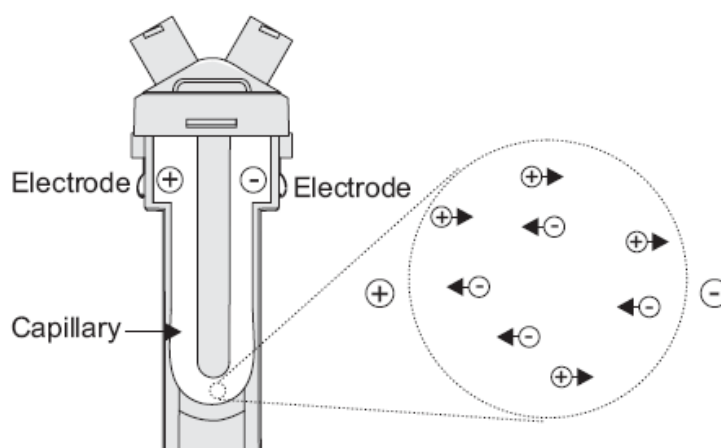
either 1.5 or 1.0.

Fig 14. Electric field is applied across an electrolyte.

Organic element analyzer[33)]

Elemental analysis on carbon, hydrogen and nitrogen is the most essential and in many cases the only investigation performed to characterize and/or prove the elemental composition of an organic sample.

For CHN determination, the organic element analyzer operates with the dynamic flash combustion of the sample. The sample under test is weighed in using a tin capsule. The required amount is 2 to 3 mg of organic material and can hardly exceed 10 mg, if inorganic matter with little carbon content is investigated. After folding the capsule (looking rather like wrapped tin foil) the sample is placed in the autosampler. The tin capsule enclosing the sample falls into the reactor chamber where excess oxygen is introduced before. At about 990 ℃ the material is "mineralized". Formation of carbonmonoxide is probable at this temperature even under these conditions of excess oxygen. The complete oxidation is reached at a

tungsten trioxide catalyst which is passed by the gaseous reaction products. The resulting mixture should thus consist of CO_2, H_2O and NO_x. But also, some excess O_2 passes the catalyst. The product gas mixture flows through a silica tube packed with copper granules. In this zone held at about 500 °C remaining oxygen is bound, and nitric/nitrous oxides are reduced. The leaving gas stream includes the analytically important species CO_2, H_2O und N_2. Eventually included SO_2 or hydrohalogenides are absorbed at appropriate traps. High purity helium (Quality 5.0) is used as carrier gas. Finally, the gas mixture is brought to a defined pressure/volume state and is passed to a gas chromatographic system. Separation of the species is done by so called zone chromatography.
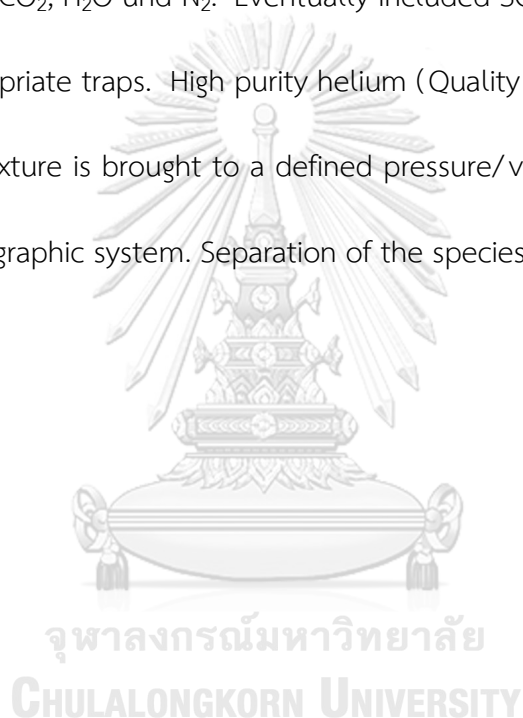
The main objective of this research

The first part was to study the effect of concentration of reactants and time on size and dispersion of silica nanoparticle in ethanol.

The second part was to study amount of MPS for chemisorbed on silica nanoparticles.

The third part was to study effects of various amount of silica nanoparticle and effects of various amount of MPS on mechanical properties of silica nanoparticles-reinforced PMMA.
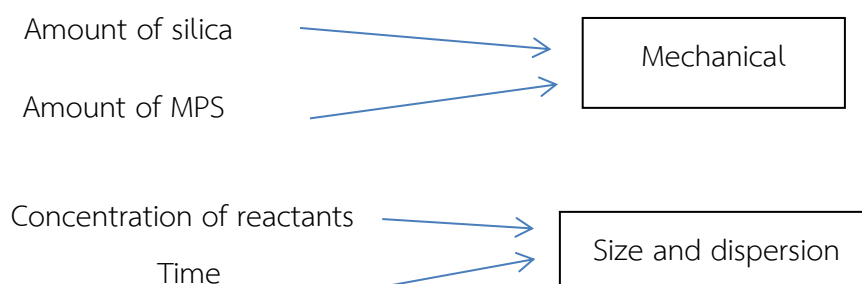
Hypotheses

H1o: The amount of silica nanoparticle has no effect on mechanical properties of silica nanoparticles-reinforced PMMA.

H1a: The amount of silica nanoparticle has effect on mechanical properties of silica nanoparticles-reinforced PMMA.

H2o: The amount of MPS has no effect on mechanical properties of silica nanoparticles-reinforced PMMA.

H2a: The amount of MPS has effect on mechanical properties of silica nanoparticles-reinforced PMMA.

Conceptual framework

Keywords

Silica Nanoparticle

Amount of chemisorbed MPS
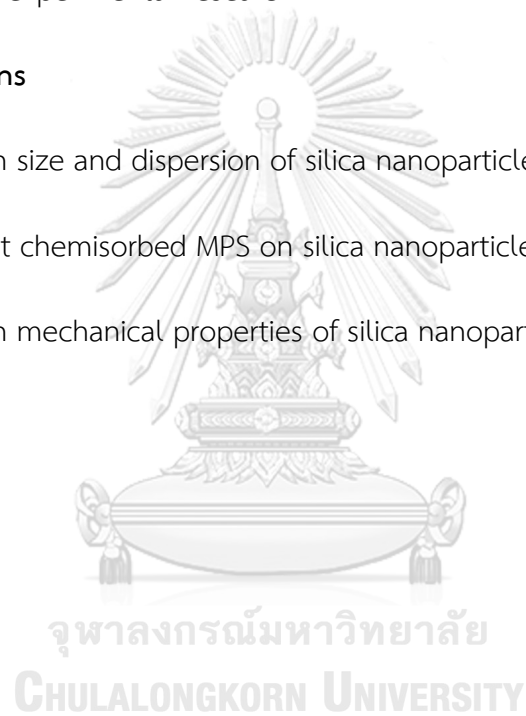
Reinforce-PMMA

Research design

Laboratory experimental research

Research questions

What the effect on size and dispersion of silica nanoparticle?

How many amount chemisorbed MPS on silica nanoparticle?

What the effect on mechanical properties of silica nanoparticle reinforced PMMA?

Materials and Methods

The effect of concentration of reactants and time on size and dispersion of silica nanoparticle.

Reagents

Tetraethoxysilane (TEOS, 98%, Sigma-aldrich), absolute ethanol (ETH, 99.9%, J.T. Baker), ammonia solution (NH3 30%, J.T. Baker), and distilled water have been used in this work. The chemicals were employed without any further purification.

Standard procedure for monodispersion silica nanoparticle

Silica nanoparticles are synthesized by using a standard procedure with experimental conditions. A quantity of 4 mL of TEOS was first dissolved in 50 mL of absolute ethanol under magnetic stirrer (Stuart, UC152) at room temperature for 10 min. Then, 1 mL of distilled water was dropped into the reaction media to facilitate hydrolysis of TEOS. After 1.5 h, 0.231 mol/L, 0.458 mol/L of ammonia solution was fed into the reaction mixture. The reaction was continued for 1, 4, 8 h, 1, 2, 3, 4, 5, 7, 9, and 30 days. The dispersion of silica nanoparticle of each group was carried out and then was characterized for TEM and dynamic light scattering. For investigation, specific surface area, the dispersion of silica nanoparticle was dried using a conventional oven (Memmert) at 70 C for 24 h. The samples were calcined at 600 C for 2 h. All groups are showed in table 2.

Table2. Demonstrate groups of specimens.

time \ Concentration	0.231 mol/L	0.458 mol/L
1 hr	1	12
4 hr	2	13
8 hr	3	14
1 day	4	15
2 days	5	16
3 days	6	17
4 days	7	18
5 days	8	19
7 days	9	20
9 days	10	21
30 days	11	22

Characterization

Transmission electron micrograph

Particle size of the samples was studied by using a transmission electron microscopy (TEM, JEOL 2011) operated at an acceleration voltage of 80 kV. One drop of suspension was evaporated on a carbon-coated copper grid.

Scanning electron micrograph

Morphological attributes of nanosilica were measured using Scanning Electron Microscope (SEM, JEOL) at an accelerating voltage of 15-20 kV. The samples were

analyzed with gold coating to improve the surface conductivity. The samples were deposited on a sample holder with a double stick conducting carbon tape.

Zeta potential

Zeta potential values of dispersion of silica nanoparticle were measured by a Zeta meter (Zetasizer Nano ZS, Malvern). The pH of the suspension was adjusted to a desired value by employing 0.1 mol/l solutions of HCl or NaOH, respectively. An average of at least three measurements for each sample was recorded.

Dynamic light scattering

Particle sizes and particle size distributions were determined from dynamic light-scattering (Zetasizer Nano ZS, Malvern) experiments by analysing the Stokes–Einstein autocorrelation function.

Specific surface area (BET)

Surface area of samples was measured by adsorption–desorption of nitrogen isotherm at 77 K on an automatic physisorption analyzer (Autosorb-1, Quantachrome). The samples were degassed overnight under vacuum at 105 $^\circ$C before measurement.

Modification of silica nanoparticles

Spherical nanosilica were prepared by the hydrolysis of tetraethoxysilane (TEOS) in ethanol (ETH), distilled water (H_2O) and ammonium hydroxide (NH_4OH). The particle size was controlled by the concentrations of TEOS, H_2O and NH_4OH in ETH, according to the relations proposed by Bogust *et al*[5]. In this study, 36 nm-size nanosilica were synthesized from the concentrations of TEOS, H_2O and NH_3 equal to

0.322, 1 and 0.233 mol/L, respectively. Eight mL of TEOS was dissolved in 100 mL of

absolute ETH under magnetic stirrer at room temperature (23±2°C) for 10 minutes.

Then, 2 mL of H_2O was dropped into the reaction media to facilitate hydrolysis of

TEOS. After 90 minutes, 1 mL of NH_4OH (catalyst) was added into the reaction mixture.

The reaction was continued for 7 days to obtain monodisperse nanosilica.

The amount of MPS used in the silanization of nanosilica was calculated by

modified Posthumus's equation[12] as follows:

$$X=m_{silica} \times MW_{MPS} \times M_{MPS} \times BET_{silica} \times 10^{-6}$$

where, X is the amount of silane in gram (g)*, m_{silica}* is the amount of silica in

gram, MW_{MPS} is the molecular weight of MPS (248.35 g/mol), M_{MPS} is the amount of

required chemisorb (6.9 µmol/m^2), BET_{silica} is the specific surface area of nanosilica (36

nm in size of nanosilica in this study has the surface area 576 m^2/g)

The nanosilica was silanized with different amounts of MPS 0, 0.061, 0.123,

0.246, 0.493, 0.987, and 1.974 g_{MPS}/g_{silica}, respectively. MPS was pre-hydrolyzed in an

aqueous solution of 80% ETH at room temperature for 1 hour. The hydrolyzed MPS

was added into the nanosilica suspension and stirred using magnetic stirrer at a

frequency of 200 rpm for 2 hour at room temperature, and then refluxed for 4 hour

at 70°C. At the end of the reaction, the mixture was allowed to cool down and divided

into two parts for analysis. The first part was dried by solvent evaporation at 50±5°C in

an oven (Memmert, GmbH, Schwabach, Germany). This resulted in a mixture of

silanized nanosilica, unreacted MPS and homocondensates of MPS, which referred to the "dried" samples. The other part was diluted with *n*-propanol triple amount of silanized nanosilica suspension. This is to improve the solubility of the homocondensated MPS. This sample was centrifuged using high speed centrifugation (Avanti® J-E, Bechman Coulter Inc., IN, USA) at 20000 rpm for 2 hour at room temperature[12]. The clear supernatant, which contains the homocondensated MPS and unreacted MPS, was decanted from the sediment. This sediment composed of nanosilica silanized with MPS. This sediment was referred to the "centrifuged" samples. Both of the dried and centrifuged samples were dried at 50±5°C in an oven for at least 16 hour.

Characteristic of silanized silica nanoparticles

Fourier Transform Infrared Spectrophotometry (FTIR)

The grafted MPS was characterized using FTIR measurements with a narrow bandpass mercury-cadmium-telluride (MCT) detector. The dried and centrifuged specimens of silanized silica nanoparticles as described above were analyzed using FTIR spectrophotometer (PerkineElmer2000). Each IR spectra were collected from 400-4000 cm^{-1} under the nitrogen purge. Prior to the measurement, 100 mg of the dried and centrifuged sample was dispersed in 1 g of KBr powder and IR spectra were taken on a PerkineElmer 2000 spectrometer.

Organic element analyzer

The carbon content on the silanized silica nanoparticle surface was analyzed to determine the chemisorbed amounts of MPS on the silica nanoparticle surface using an organic element analyzer (Thermo Scientific™ FLASH 2000). The amounts of carbon were calculated the content of the MPS. It was determined by number of carbon element in each MPS molecule; one molecule of MPS composed of 7 atoms of carbon. Surface coverage (*C*) was calculated, as follows:

$$C = M_{MPS} \times N_A \times 10^{-18}$$

where, *C* is surface coverage (molecule/nm^2), *M_{MPS} is amount of MPS on silica nanoparticle* (μmol/m^2= μmol$\times 10^{-18}$/ nm^2), *N_A is Avogadro number (6.03$\times 10^{23}$ molecule/mol).*

Flexural strength (FS) and Flexural modulus (FM) of nanosilica reinforced PMMA denture base

The effect on the amount of nanosilica

The resulted from elemental analysis and FTIR indicated that 0.246 g_{MPS}/g_{silica} created a monolayer chemisorbed on nanosilica. Therefore, the silanized nanosilica of 0.246 g_{MPS}/g_{silica} was used in this study. The silanized nanosilica in the specimens were divided into 6 groups: 0.25, 0.5, 1, 5, 10 and 15 % (w/w), respectively. Specimens of PMMA without nanosilica served as control group. Eight specimens for each group were prepared for the flexural strength test. A heat-polymerized PMMA (Triplex hot, Ivoclar Vivadent AG, Schaan, Liechtenstein) was used in this study. The nanosilica silanized

with 0.246 g_{MPS}/g_{silica} with 6 different amounts of nanosilica were mixed with the monomer of PMMA by weight ratio using a rotor stator mixer 3000 rpm 10 minutes to form homogeneous suspension (Fig. 15). This is referred to the "modified monomer". The silicone template was created using metal mold (Fig. 16). The ratio of PMMA-based powder and modified monomer of each 6 groups were mixed at a 23.4 g powder and 10 mL modified monomer. After the dough stage, the mixture was placed in the flask, pressed and heat-polymerized with heat up to 100°C and let boil for 45 minutes (Fig. 17). Subsequently, after the flask cooled to room temperature, the specimens were deflasked.

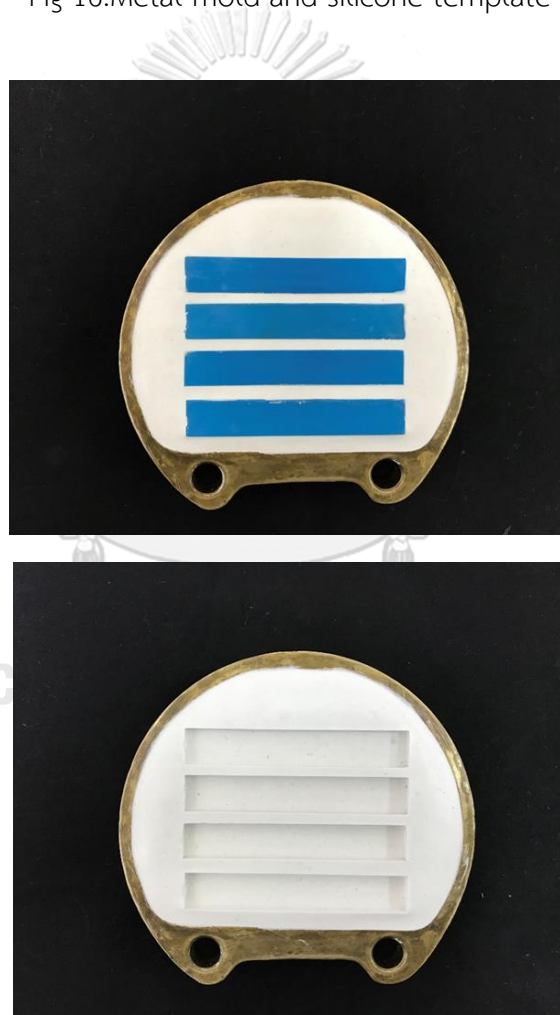Fig 15. Rotor stator mixer

Fig 16.Metal mold and silicone template

Fig 17. Flasking

The effect of the MPS amount

The 1% (w/w) amount of nanosilica was selected from the effect of amount of nanosilica mentioned above in this part. The specimens were divided into 6 groups according to the different amounts of MPS 0, 0.061, 0.123, 0.246, 0.493, 0.987, and 1.974 g_{MPS}/g_{silica}, respectively. The FS and FM values of control and 0.246 g_{MPS}/g_{silica} of 1% (w/w) were the same as the amount of nanosilica part. Fabrications of specimens of these groups for FS and FM test were the same as aforementioned in the effect on the amount of nanosilica groups.

Flexural strength and Flexural modulus test

FS was determined using a three-point bending test according to (ISO 20795-1:2013)[34]. The bar-shaped specimens, 10 mm wide, 64 mm long, 3.3mm thick, were fabricated following a conventional compressive process and polished with #500, #1000, #1200 wet silicon carbide paper using a polishing machine (Nano2000, Buehler, AZ, USA) to achieve the required dimensions of 10.0±0.2×64.0×3.2±0.2 mm (Fig. 18). To minimize edge failure in the bar specimens during flexural testing, edge chamfer was prepared with #1000 wet silicon carbide paper using a polishing machine. The specimens were immersed in 37°C deionized water for 50±2 hour prior to the three-point bending test. The width and thickness of each specimen were measured with a digital micrometer (Mitutoyo IP65, Mitutoyo Corporation, Kanagawa, Japan). A three-point bending test, with a support span of 50 mm, a cross-head speed of 5 mm/min and 500 N load cells, was conducted at room temperature using a universal testing

machine (EX-S500N, Shimadzu, Kyoto, Japan) (Fig. 19). The FS and FM were calculated

using software (Trapezium II, Shimadzu, Kyoto, Japan). FS (σ) and FM (E) = were

calculated by following equation:

$$\sigma = 3FL/2bh^2$$

$$E = L3m/4bh^3$$

where, F is the maximum load during the flexural test (N), L is the span distance (50.0

mm), b is the width of the specimen, h is the height of the specimen, and m is the

gradient (slope) of the initial straight-line portion of the load deflection curve (N/mm).
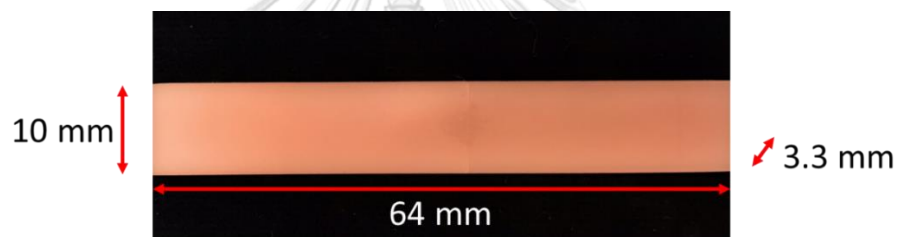
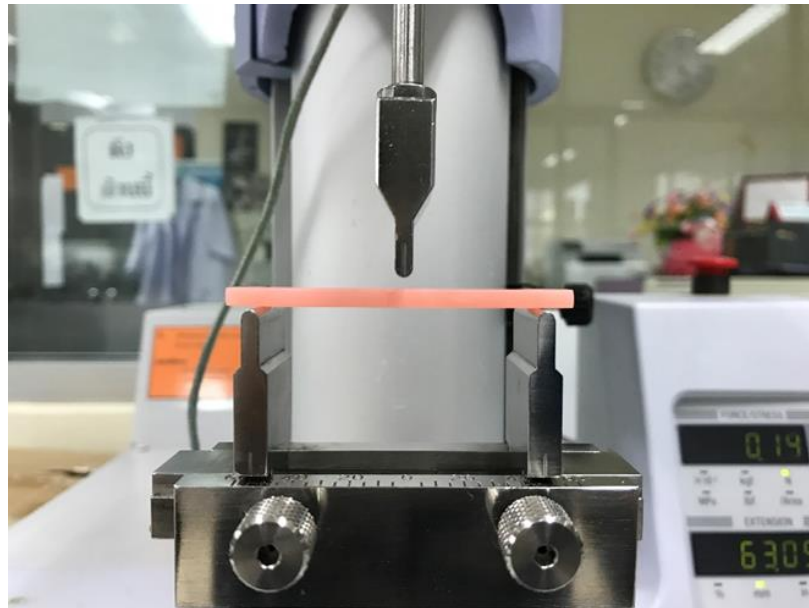Fig 18. Specimen for flexural strength test

Fig 19. Flexural strength test

Fracture toughness test

FT was determined using a three-point bending test according to (ISO 20795-1:2013)[19,34]. The bar-shaped specimens, 8 mm height, 39 mm long, 4 mm width, pre-crack 3 mm, 0.1-0.4 mm crack length, were fabricated following a conventional compressive process and polished with # 500, #1000, #1200 wet silicon carbide paper using a polishing machine (Nano2000, Buehler, AZ, USA) to achieve the required dimensions of 8.0±0.2×39.0×4.0±0.2 mm (Fig. 20). Pre-crack was created to the depth of 3.0±0.2 mm using low speed cutting machine (IsoMet 1000, Buehler, IL, USA) (Fig. 21). The razor blade (Feather-Cut, FEATHER Safety Razor Co. Ltd, Gifu, Japan) was set of the bottom of the pre-crack and the sharp notch was cut with hand in a back and forth sliding motion (Fig. 22). The specimens were immersed in 37ºC deionized water

for 7 days±2 hour prior to the three-point bending test. The width and height of each specimen were measured with a digital micrometer (Mitutoyo IP65, Mitutoyo Corporation, Kanagawa, Japan). A three-point bending test, with a support span of 32 mm, a cross-head speed of 1 mm/min and 500 N load cells, was conducted at room temperature using a universal testing machine (EX-S500N, Shimadzu, Kyoto, Japan) (Fig. 23). The test was considered finished when the current load dropped 1.0±0.2 N from the maximum load. The maximum load was recorded in newtons. Optical microscope with micrometer scale was used to measure the total length of the crack. The total length of the crack was measured using Image J software (Fig. 24). FT (K_{max}) was calculated by following equation:

$$K_{max}=fP_{max}l_t\sqrt{10^{-3}}/(b_t h_t^{3/2})$$

where, f is a geometrical function dependent on x:

$$f(x)=3x^{1/2}[1.99-x(1-x)(2.15-3.93x+2.7x^2)]/[2(1+2x)(1-x)^{3/2}]$$

$x=a/h_t$, P_{max} is maximum load on specimen, in newtons, l_t is a span distance (32 mm), b_t is a width of the specimen, h_t is a height of the specimen, a is a total crack length.
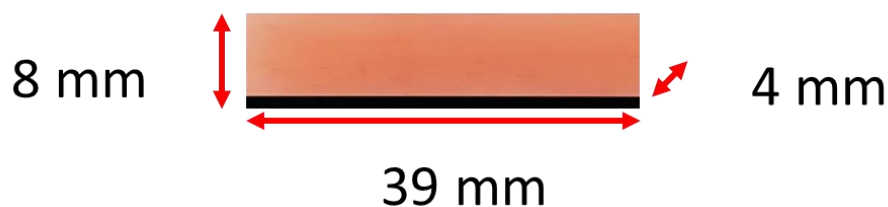

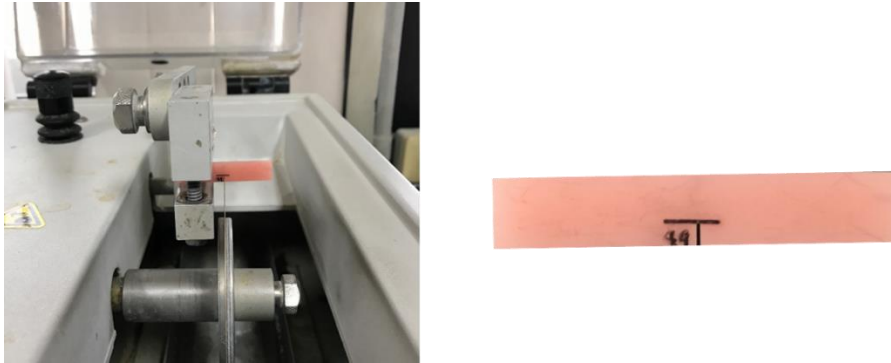Fig 20. Dimension specimen for fracture toughness test
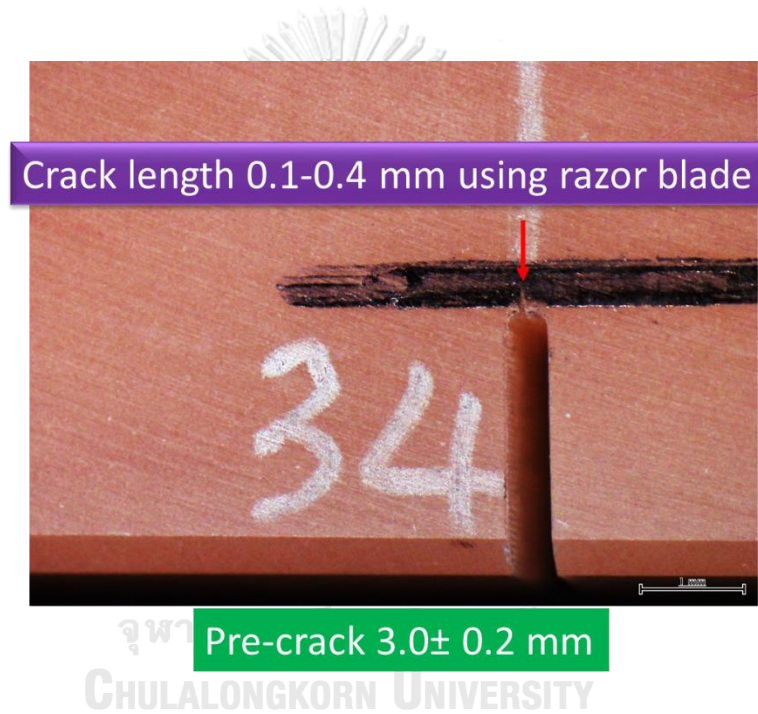
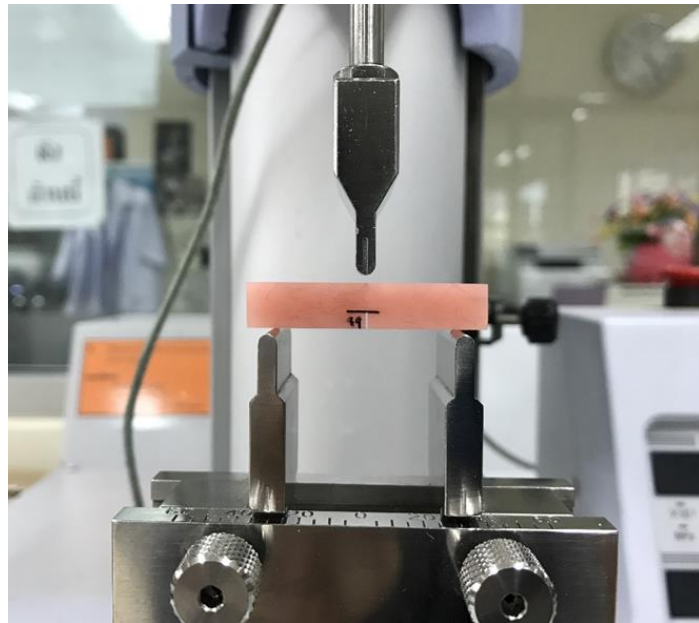Fig 21. Pre-crack using low speed cutting machine

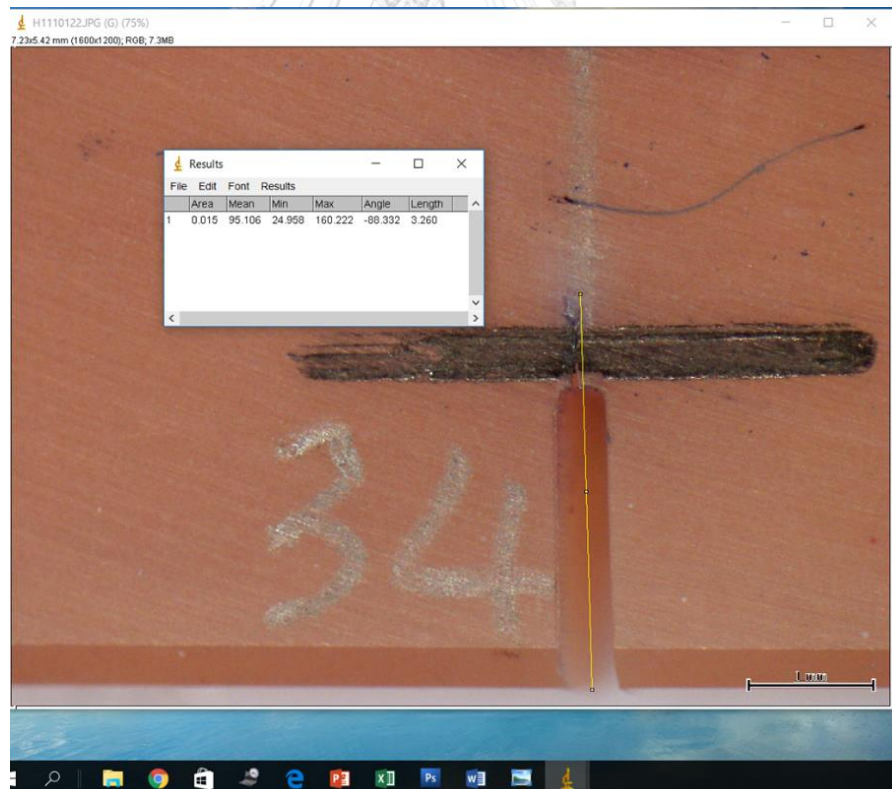Fig 22. Crack length

Fig 23. Fracture toughness test

Fig 24. Measurement of total crack length

Scanning Electron Microscopy (SEM)

The fractured surface of pure PMMA, 1% (w/w) of 0, 0.061, 0.123, 0.493, 0.987, and 1.974 g_{MPS}/g_{silica} silanized nanosilica groups after three-point bending of FT test were observed by a field emission scanning electron microscope (JEOL JSM7800F, JEOL, Tokyo, Japan). The fractured surfaces of specimens after the FT test were carbon coated. The primary electron beam energy was operated at 5 kV for each specimen. Backscattered electrons were used to create backscatter diffraction image.

Transmission Electron Microscopy (TEM)

The morphology and distribution of nanosilica reinforced PMMA denture base were performed using a TEM operated at an acceleration voltage of 120 kV. Thin sections, approximately 200 nm in thickness, were prepared using a ultramicrotome (Leica EM UC7, Leica Microsystems, Vienna, Austria) equipped with a diamond knife at room temperature without any chemical etching.

Color measurement

A spectrophotometer (Ultrascan XE, Hunter Lab Inc, VA, USA) was used to measure the color changes with the L*a*b* color system (CIE). This system is based on three parameters for defining color: L*, a*, and b *. L* represents lightness, a* represents red-green, and b* represents yellow-blue. The color difference (ΔE) was calculated based on the L*, a*, and b* on black background between the control and experimental group using the following equation:

$$\Delta E = [(L^*_1 - L^*_2)^2 + (a^*_1 - a^*_2)^2 + (b^*_1 - b^*_2)^2]^{1/2}$$

where the subscripts 1 and 2 refer to the color coordinates control and experimental groups, respectively. A high ΔE value indicates a large color difference. Three measurements were made on each specimen, and the average value was recorded.

Statistical analysis

The FS, FM, ΔE of different amount of silanized nanosilica and FT, ΔE of different amounts of MPS were separately analyzed with one-way ANOVA and Tukey's post-hoc comparison (SPSS ver. 20, IBM, NY, USA). The significance level was set at α=0.05.

จุฬาลงกรณ์มหาวิทยาลัย
CHULALONGKORN UNIVERSITY

RESULTS

TEM images revealed a narrow size and shape distribution of the experimental nanosilica with low aggregation and agglomeration (Fig. 25). The result from DLS analysis showed 36 nm in size with good distribution (Fig. 26). The specific surface area from automatic physisorption analyzer of experimental nanosilica was 576 m^2/g.

FTIR spectra of dried samples showed the absorption peaks at 2800-3000, 3660, 1702, 1631 cm^{-1} attributing to hydrocarbon chain, hydrogen bond, carbonyl group and vinyl group, respectively (Fig. 27A)[10, 35]. Nanosilica prior to surface modification, the hydrocarbon chains, carbonyl group, and vinyl group were not detected. The intensity of absorption bands at 2800-3000, 1702, and 1631 cm^{-1} of dried samples incrementally increased from 0.061 to 1.974 g_{MPS}/g_{silica} groups. The absorption bands of centrifuged sample were the same as dried sample with intensity of absorption band at 2800-3000, 1702, and 1631 cm^{-1} reached the plateau at 0.246 g_{MPS}/g_{silica} group (Fig. 27B).

The adsorbed amounts of MPS on the nanosilica surface from elemental analysis of carbon in dried groups were from 0.43-8.39 $\mu mol/m^2$, while the centrifuged groups were from 0.49-3.11 $\mu mol/m^2$ (Fig. 28). Chemisorbed MPS molecules on nanosilica surface were from 0.26-5.05 molecule/nm^2 in dried groups and 0.30-1.87 molecule/nm^2 in centrifuged groups (Fig. 28).

The FS of different amounts of nanosilica groups were from 85.2-105.8 MPa (Table 3). The FM of different amounts of nanosilica groups were from 2.4-3.1 GPa

(Table 3). One-way ANOVA of FS and FM revealed significant difference among groups. Tukey-HSD indicated that FS and FM of 1% (w/w) of nanosilica of 0.246 g_{MPS}/g_{silica} group was significantly higher than those of the others. The FS of different MPS amounts groups were from 80.3-105.8 MPa (Table 4). The FM of different MPS amounts groups were from 2.4-3.0 GPa (Table 4). One-way ANOVA of FS and FM of different MPS amounts revealed significant difference among groups. The Tukey-HSD indicated that 0.246 g_{MPS}/g_{silica} amount of MPS of 1% (w/w) of amount of nanosilica group was significantly higher than those of the others. The FT of different MPS amounts groups were from 1.6-2.4 MPa.m$^{1/2}$ (Table 4). One-way ANOVA revealed significant difference among groups and the Tukey-HSD indicated that 0.246 g_{MPS}/g_{silica} amount of MPS of 1% (w/w) nanosilica group was significantly higher than those of the others.

The ΔE of different amounts of nanosilica groups were from 0.7-1.8 (Table 3). One-way ANOVA revealed significant difference among groups and the Tukey-HSD indicated that 15% (w/w) of nanosilica of 0.246 g_{MPS}/g_{silica} group was significantly higher than those of the others. The ΔE of different MPS amounts were from 0.6-0.8 (Table 4). One-way ANOVA of revealed no significant difference among groups.
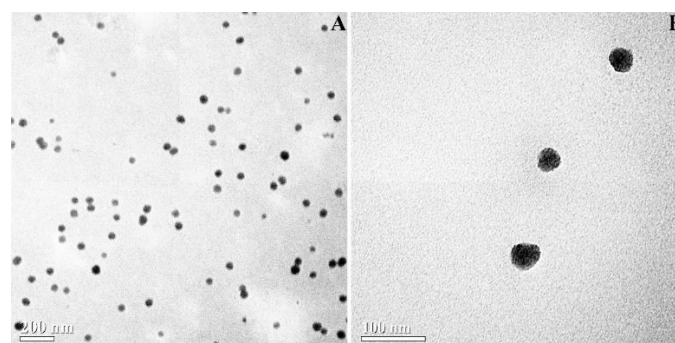
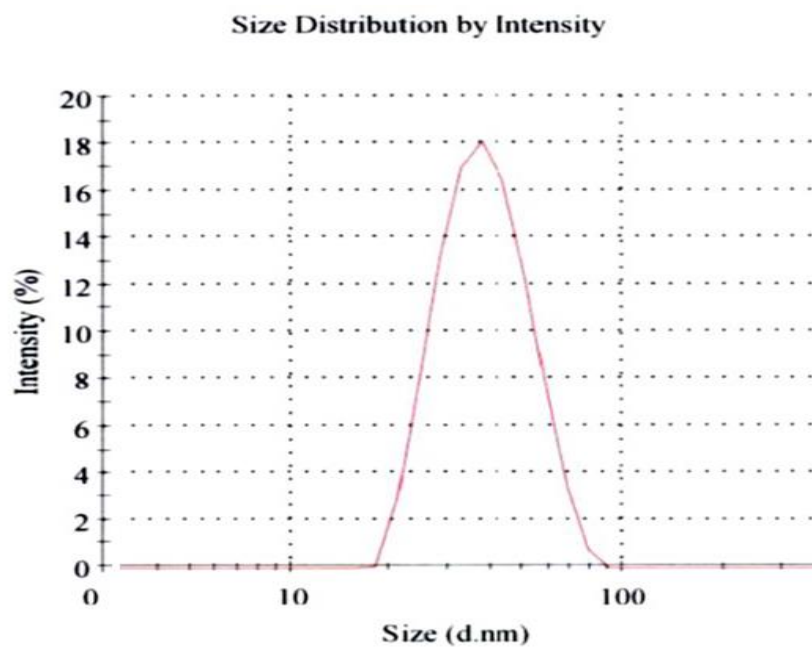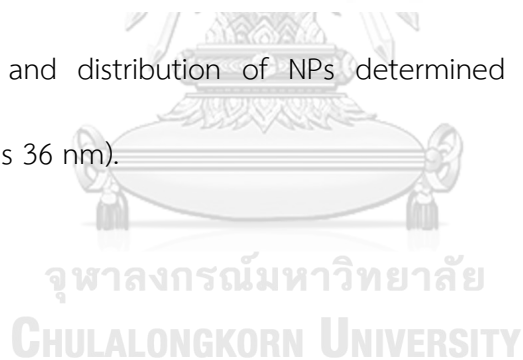Fig. 25 TEM images of NP size and distribution. A: 20k magnification, B: 40k magnification.

Size Distribution by Intensity

Fig. 26 NPs size and distribution of NPs determined by DLS (average size of experimental NPs is 36 nm).

จุฬาลงกรณ์มหาวิทยาลัย

CHULALONGKORN UNIVERSITY
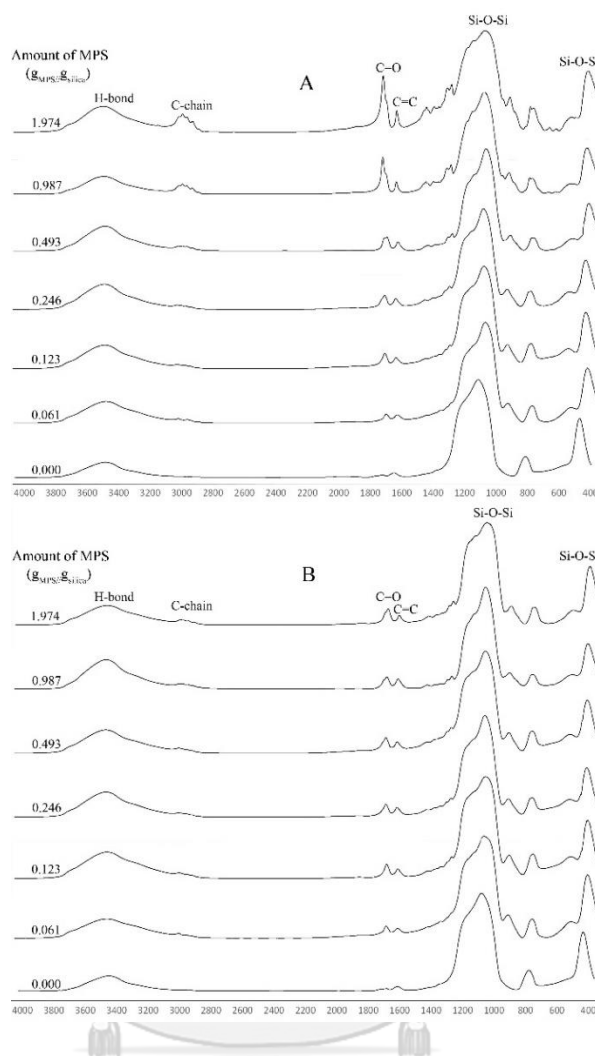
Fig. 27 FTIR spectra of A: dried samples showing absorption peaks at 3434, 2986, 1702, 1631, 1091, and 462 cm^{-1} representing hydrogen bonds, hydrocarbon chains, carbonyl groups, vinyl group, Si-O-Si (symmetrical stretch), and Si-O-Si (rocking), respectively. B: The FTIR spectra of centrifuged samples shows that the absorption peaks at 3434, 2986, 1702, 1631, 1091, and 462 cm^{-1} reached plateau in the 0.246 g$_{MPS}$/g$_{silica}$ group.
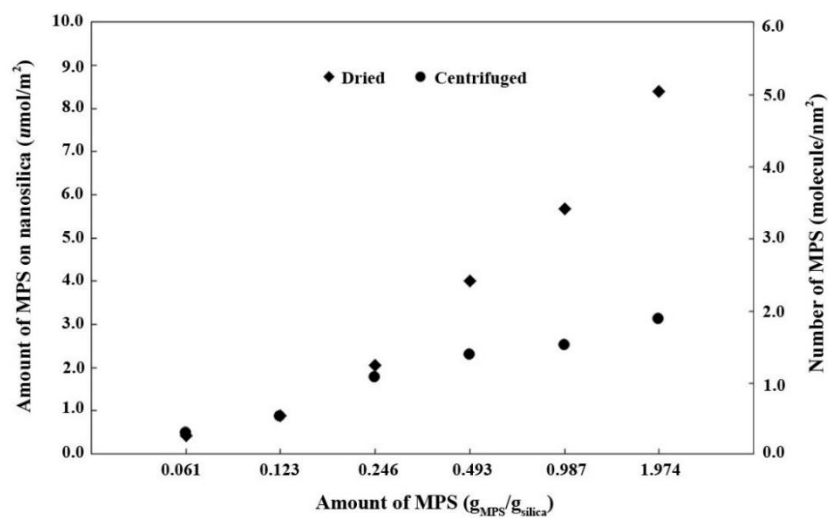
Fig. 28 Amount of MPS on the nanosilica surface and number of molecules of MPS on the nanosilica surface as determined by elemental analysis in the dried groups and centrifuged groups.
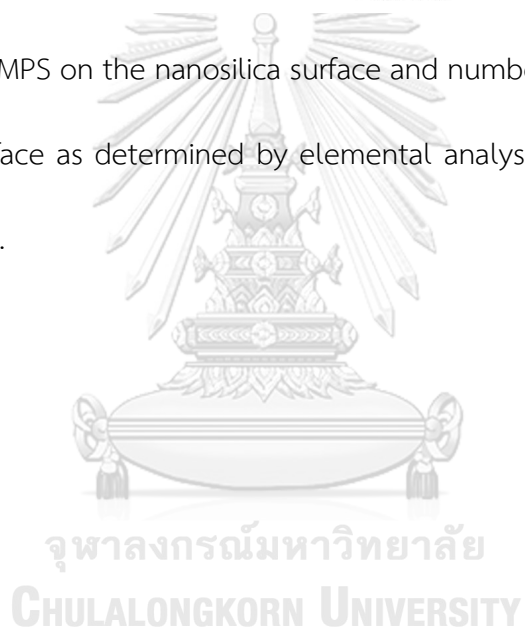
Table 3 Flexural strength, flexural modulus, and ΔE of 0.246 gMPS/gsilica with different amount of nanosilica groups.

Conditions	Flexural strength (MPa)	Flexural modulus (GPa)	ΔE
control (no filler)	85.2(3.8)[a]	2.4(0.1)[a]	–
0.25% NP	93.4(4.2)[b]	2.7(0.1)[b]	0.8(0.2)[a]
0.5% NP	94.5(3.1)[b]	2.7(0.0)[b]	0.7(0.1)[a]
1% NP	105.8(3.4)[c]	3.0(0.0)[c]	0.8(0.1)[a]
5% NP	97.0(2.5)[b]	2.9(0.1)[c]	1.4(0.1)[b]
10% NP	89.3(3.6)[a,b]	3.1(0.1)[c]	1.6(0.1)[b,c]
15% NP	84.3(3.6)[a]	3.1(0.1)[c]	1.8(0.2)[c]

% (w/w)

Mean values (n=8) and standard deviations in parentheses.

For each property, values denoted with same letters are not significantly different (p>0.05).

Table 4 Flexural strength, flexural modulus, fracture toughness, and ΔE of 1% amount of nanosilica with different amount of MPS groups.

Conditions	Flexural strength (MPa)	Flexural modulus (GPa)	Fracture toughness (MPa·m$^{1/2}$)	ΔE
control (no filler)	85.2(3.8)[a]	2.4(0.1)[a]	1.9(0.2)[a,b]	–
0.000 (unsilanized)	81.0(5.0)[a]	2.6(0.1)[a]	1.6(0.4)[a]	0.6(0.1)[a]
0.061	80.3(5.4)[a]	2.4(0.0)[a]	1.9(0.3)[a,b]	0.7(0.1)[a]
0.123	97.1(1.6)[b]	2.7(0.1)[b]	2.0(0.3)[b]	0.6(0.1)[a]
0.246	105.8(3.4)[c]	3.0(0.0)[c]	2.4(0.3)[c]	0.8(0.1)[a]
0.493	98.2(3.3)[b]	2.6(0.0)[b]	2.0(0.3)[b]	0.8(0.2)[a]
0.987	93.9(3.6)[b]	2.6(0.0)[b]	1.9(0.2)[a,b]	0.7(0.1)[a]
1.974	84.6(4.0)[a]	2.3(0.1)[a]	1.6(0.2)[a]	0.6(0.1)[a]

Amount of MPS (gmps/gsilica)

Mean values (n=8) and standard deviations in parentheses.

For each property, values denoted with same letters are not significantly different (p>0.05).

จุฬาลงกรณ์มหาวิทยาลัย

CHULALONGKORN UNIVERSITY

DISCUSSION

The adsorption bands of silanized nanosilica at 3434 cm^{-1}, 2986 cm^{-1}, 1702 cm^{-1}, 1631 cm^{-1}, 1091 cm^{-1} and 462 cm^{-1} attribute to hydrogen bond, hydrocarbon, carbonyl groups, vinyl group, Si-O-Si (symmetrical stretch), and Si-O-Si (rocking), respectively[13] (Fig. 27). The result indicated that the silanization process in this studwas effective.

The FTIR spectra in dried groups of the nanosilica as a function of MPS amount showed the intensity of 2986 cm^{-1}, 1702 cm^{-1}, 1631 cm^{-1} band which corresponded to the chemisorbed and physisorbed of MPS which increased gradually from 0.061 to 1.974 g$_{MPS}$/g$_{silica}$ groups (Fig. 27A). In centrifuged groups, the intensity of adsorption band reached the plateau at 0.246 g$_{MPS}$/g$_{silica}$ group (Fig. 27B). These spectra of the centrifuged groups after 0.246 g$_{MPS}$/g$_{silica}$ confirmed the complete removal of physisorbed MPS by n-propanol and centrifugation at 20000 rpm.

In dried group, the amount of physisorbed and chemisorbed increased with the increasing amount of MPS. On the other hand, in centrifuged groups, the amount of chemisorbed MPS increased until the amount of MPS reached 0.246 g$_{MPS}$/g$_{silica}$. At this point, the chemisorbed MPS reached the plateau (Fig. 28). Therefore, the optimal amount of chemisorbed MPS on the nanosilica was 1.77 μmol/m^2. The plateau phase of chemisorbed layer probably occurred because of the steric hindrance of the organic group in the MPS molecule[36]. The chemisorbed amount of 1.77 μmol on 1 m^2 of

nanosilica surface in this study corresponded to approximately 1.07 MPS molecules on 1 nm^2 of nanosilica surface. The silica has 3 or 4 Si-OH groups for 1 nm^2 of nanosilica surface[37]; therefore, unreacted Si-OH groups on the nanosilica still remain. The chemisorbed amount of MPS of this study was 7 times lower than theoretically computation suggested by Arkles (12.82 µmol/m^2). In contrast to the study of Arksornnukit *et al.*[24], they reported 12.88 µmol/m^2 for monolayer coverage and 7.7 MPS molecule on 1 nm^2 of silica based on Arkles's equation. This differences is probably due to the difference in size of silica. The bigger size of silica provides adequate space for adsorption of silane oligomer. The condensation reaction of the silane molecules on the silica surface simultaneously occurs along with condensation among the silane molecules with a slower rate. Therefore, the higher molecular weight molecules such as tetramer, trimer or dimer would be chemisorbed on the silica surface.

The orientation of MPS molecule on nanosilica was parallel or perpendicular. The parallel orientation indicates that one MPS molecule react with 2 Si-OH molecules on nanosilica surface resulted in hydrogen bond between C=O of MPS and Si-OH on nanosilica surface and siloxane bond between Si-OH of MPS and Si-OH on nanosilica surface. The perpendicular orientation indicates that one molecule of MPS reacts with one Si-OH molecule resulted in siloxane bond between Si-OH of MPS and Si-OH on nanosilica surface[36]. The behavior of the C=O band in MPS molecule indicates that the orientation behavior of MPS depends upon the number of chemisorbed MPS

molecules on 1 nm^2 nanosilica surface. The result of this study also showed that the parallel orientation of MPS adsorption between 0.61-1.07 molecule on 1 nm^2 which showed C=O band at 1702 cm^{-1} representing hydrogen bond C=O group with Si-OH groups. While, the groups which exceeded 1.07 molecule on 1 nm^2, a new C=O band at 1720 cm^{-1} appeared due to the free C=O (Fig. 29)[10, 13]. This results indicated that MPS molecules oriented perpendicular to the nanosilica surface. MPS molecules can be further forced to establish the chemisorption to the nanosilica beyond the plateau phase which was demonstated in Fig. 28. Excess amount of MPS will likely transform the direction of adsorbed MPS molecules at nanosilica surface from parallel to perpendicular. As a result, the amount of MPS per surface area of nanosilica increased from 1.07 to 1.87 molecule/nm^2.

The FS and FM results showed differences in the amount of nanosilica content (Table 3). Therefore, the null hypothesis that there would be no differences in the FS and FM of PMMA denture base reinforced with various amounts of nanosilica was rejected. The FS and FM of the PMMA containing silanized nanosilica steadily increased from groups 0.25 to 1% (w/w). The increase amount of the silanized nanosilica resulted in more covalent linkages at the interface between nanosilica and the PMMA matrix. However, when the nanosilica amount exceeded 1% (w/w), the interparticle spacing decreased which created the higher chance for agglomeration (Fig. 30A-C). This generated stress concentration at agglomerated particle and deteriorated the mechanical properties of PMMA matrix[38, 39]. Thus, the FS in groups containing silanized

nanosilica over 1% (w/w) showed the reduction which showed almost no change in FM. The result of the present study found that optimum load value of 36 nm in diameter of nanosilica content was 1% (w/w) which created the homogeneous dispersion of silanized nanosilica in PMMA matrix resulted in a higher value in both FS and FM (Fig. 30D).

The FS, FM, and FT results showed the differences in the amount of MPS (Table 4). Therefore, the null hypotheses that there would be no differences in the FS, FM and FT of PMMA denture base reinforced with various amounts of silanized on nanosilica were rejected. The FS, FM and FT of the PMMA containing silanized nanosilica was greater than that of pure polymer and the PMMA containing unsilanized nanosilica. PMMA containing of 0.246 g_{MPS}/g_{silica} silanized on nanosilica showed the highest FS, FM and FT. The results from elemental analysis showed that monolayer chemisorbed occurred in 0.246 g_{MPS}/g_{silica} group. The monolayer chemisorbed is defined as MPS reacts with the silanol groups on the silica surface and forms the siloxane bridge (Si-O-Si), synchronously provided the reactive double bond from MPS molecule on the surface, which can later react with the PMMA monomer during the polymerization. As a result, MPS creates the covalent linkages between the nanoparticles and the polymer matrix[2, 9, 10]. The covalent bond between nanosilica and PMMA provided adequate stress transfer from the matrix to nanosilica[17]. For PMMA containing unsilanized nanosilica, the compatibility of the interface between the inorganic silica and the organic polymer matrix is poor, and the chemical interaction,

either Van der waal's forces or hydrogen bonds, is also weak[2]. When a force imposes

on the composites, a stress will be concentrated at the interface between fillers and

the matrix. The stress cannot be effectively transferred, therefore, it will cause cracks,

and finally induce material failure resulting in the lowest value in FS, FM and FT in

PMMA containing unsilanized nanosilica groups. However, amount of MPS is also an

important factor. The FS, FM and FT of 0.061 and 0.123 g_{MPS}/g_{silica} groups were lower

than that of 0.246 g_{MPS}/g_{silica} group. This attributed to the incomplete surface coverage

of nanosilica by MPS molecule. The remaining Si-OH on silica surface cannot react with

PMMA, which creates poor interface between PMMA and silica surface. Moreover,

0.493, 0.987, and 1.974 g_{MPS}/g_{silica} groups which have physisorbed layer on the

nanosilica as demonstated in elemental ananlysis (Fig. 28) also showed a lower FS, FM

and FT. This resulted from the physisorbed layer which contained weak Van der waal's

forces and hydrogen bond. SEM image of fractured surface reflected the information

about the cause and location of failure in details (Fig. 31). This can also explain the

reinforcement mechanism of particles for composites. Fractured surface for the pure

PMMA matrix revealed a brittle behavior characterized by the large smooth area (Fig.

31A1). The higher magnification shows direction of crack propagation as a river lines

(Fig. 31A2)[40]. This indicates a weak resistance to the crack propagation, and minimal

energy required to fracture the specimen. The 1% (w/w) unsilanized nanosilica

reinforced PMMA denture base showed smooth fractured surface (Fig. 31B1),

agglomeration and uncoverage of nanosilica (Fig. 31B2) that indicated no chemical

bond between the inorganic silica and the organic resin matrix[38]. The fractured surface

of 0.061 and 0.123 g_{MPS}/g_{silica} MPS amount groups showed rougher fractured surface

and cavitation on fractured surface (Fig 31C, 31D). This indicated tough behavior of

material. The PMMA containing 1% (w/w) of 0.246 g_{MPS}/g_{silica} MPS amount of silanized

nanosilina revealed a tougher behavior characterized by the most rough fractured

surface, out of the plane cracking, cavitation on fractured surface (Fig. 31E1), and

debonding/pullout of nanosilica (Fig. 31E2). This requires additional energy to destruct

the materials. Therefore, the increase in both FS and FT was obtained. While, the

PMMA containing 1% (w/w) of 0.493, 0.987, and 1.974 g_{MPS}/g_{silica} MPS amount groups

revealed ductile behavior characterized by large cavitation on fracture surface (Fig 31F,

31G, 31H). The excess adsorbed amount of MPS of these groups created a physisorbed

layer on nanosilica surface resulted in crack propagation along physisorbed layer (Fig

31F2, 31G2, 31H2). The results of FT confirmed that the maximum toughtening

mechanism of nanosilica reinforced PMMA denture base resulted from monolayer

chemisorbed . The monolayer chemisorbed interface is an important factor for

toughtening mechanism of nanocomposite material. Cracks encounter particles as

obstacles, which deviate and branch the crack front. In addition, a large amount of

energy may also be consumed at the particle/matrix interface under the strong

bonding conditions as indicated in the result (Fig. 31E)[16, 41].

Previous studies showed material reinforcement when the nano-sized filler

reached 5%[2,16]. In contrast, the present study demonstrated that with a chemisorbed

MPS monolayer on the NP surface, the PMMA denture base could be reinforced using only 1% NPs.

ΔE between the groups were evaluated using the perceptibility threshold (PT) and acceptability threshold (AT). Several studies used ΔE = 1.0 as the threshold at which 50% of observers can distinguish the color difference between 2 objects (PT) and ΔE=3.7 as the threshold at which 50% of observers accepted the color difference clinically (AT)[42-44]. The ΔE values of 0.246 g_{MPS}/g_{silica} of 0.25-15% amount of silanized NP groups and 0-1.974 g_{MPS}/g_{silica} of 1% amount of silanized NP groups of NPs reinforced PMMA denture base ranged from 0.6-1.8. These results indicated that the increasing amounts of silanized NP and amount of MPS silanized on NPs in PMMA denture base affected the color of the material; however, the difference from pure PMMA was within the AT. This is likely due to the refractive index of NP (1.45) which is very close to those of MPS and PMMA denture base[22].
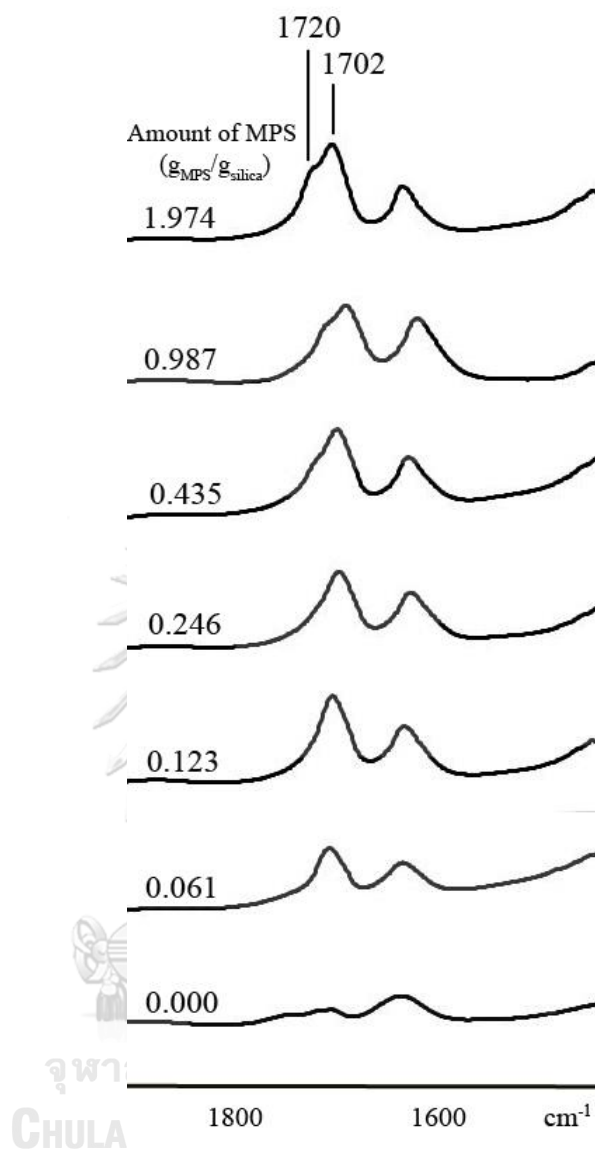
Fig. 29 The 1800-1600 cm^{-1} interval showing the location of the C=O peak at 1702 cm^{-1}. This peak reached plateau at 0.246 g$_{MPS}$/g$_{silica}$. Above this MPS amount, a peak at 1720 cm^{-1} is observed. The height of this peaked increases as the MPS amount increases.
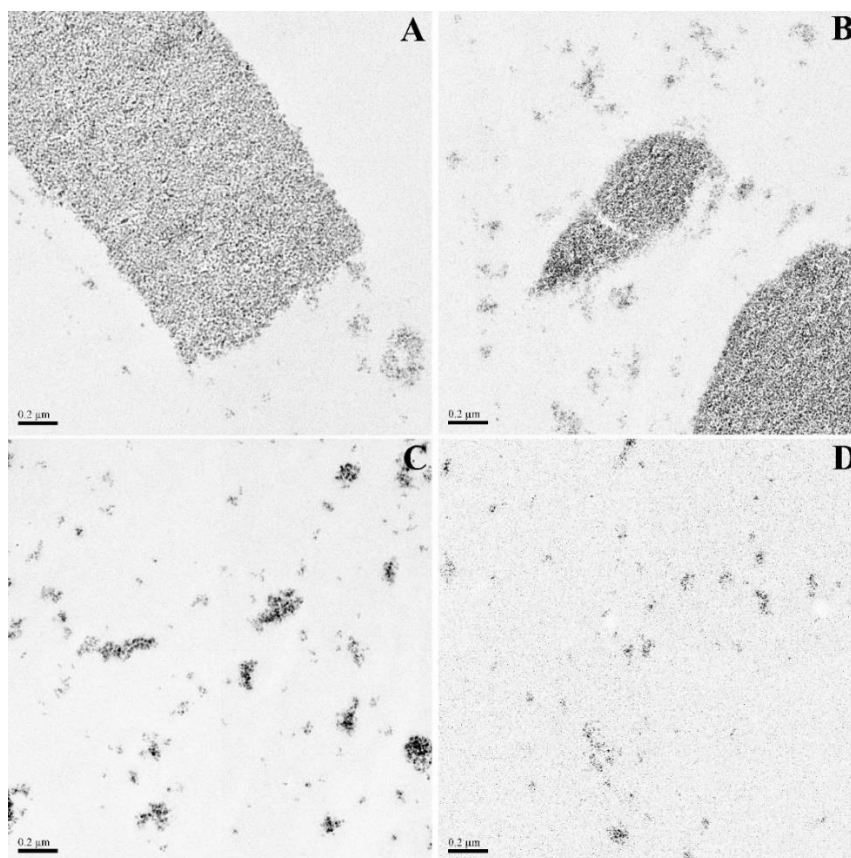
Fig. 30 Representative TEM images (9.6k magnification) of PMMA containing 0.246 g_{MPS}/g_{silica} silanized nanosilica. A: The highly agglomerated of nanosilica of 15%, B: 10% (w/w) PMMA, C: The slightly agglomerated of nanosilica of 5% (w/w) of PMMA, D: The homogeneous dispersion of silanized nanosilica 1% (w/w) of PMMA.
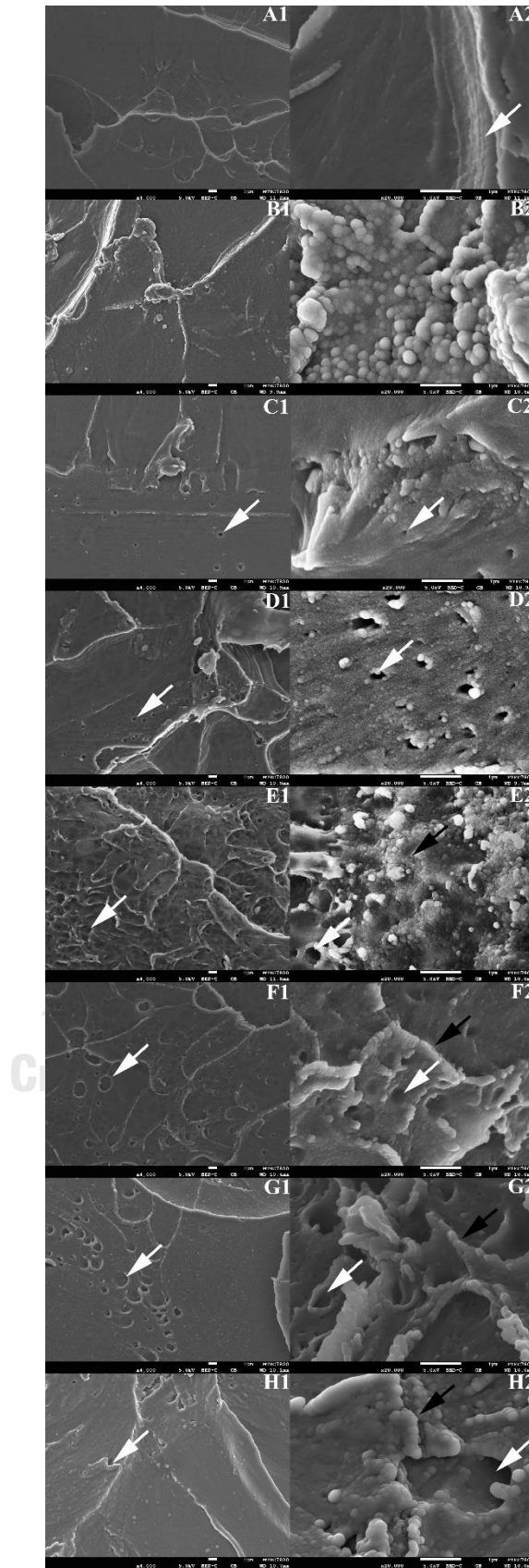
Fig. 31A-H Representative SEM images the fractured FT specimen surfaces. A: Pure PMMA, A1: The smooth fractured surface, A2: White arrow showed the river lines, B: 1% (w/w) unsilanized nanosilica, B1: The smooth fractured surface, B2: White arrow showed agglomeration and uncoverage of nanosilica, C: 1% (w/w) 0.061 MPS amount, D: 1% (w/w) 0.123 MPS amount, C1, C2, D1, D2: The rougher fractured surface. White arrows showed cavitation on fractured surface. E: 1% (w/w) 0.246 MPS amount, E1: The roughest fractured surface, E2: Black arrow showed the nanosilica pullout and white arrow showed cavitation on fractured surface, F: 1% (w/w) 0.493 MPS amount, G: 1% (w/w) 0.987 MPS amount, H: 1% (w/w) 1.974 MPS amount, F-H: White arrows showed large cavitation and black arrows showed crack propagation along physisorbed layer of silanized nanosilica. 1: 4k magnification, 2: 20k magnification.

CONCLUSIONS

Within the limitations of this study, it was concluded that the chemisorbed monolayer amount of MPS on the 36-nm in diameter spherical NPs was 1.77 μmol/m^2. The number of MPS molecules in the chemisorbed monolayer was 1.07 molecule/nm^2. Arkles's equation is not applicable in calculating the chemisorbed amount of silane on NPs. The PMMA denture base reinforced with 0.246 g_{MPS}/g_{silica} of 1% amount of silanized NPs provided the highest FS, FM, and FT which was clinically acceptable ΔE.

REFERENCES

1.   Ashton H. The Incorporation of Nanomaterials into Polymer Media. Polymer Nanocomposites Handbook: CRC Press; 2009.

2.   Du M, Zheng Y. Modification of silica nanoparticles and their application in UDMA dental polymeric composites. Polymer Composites 2007;28(2):198-207.

3.   Judeinstein P, Sanchez C. Hybrid organic-inorganic materials: a land of multidisciplinarity. Journal of Materials Chemistry 1996;6(4):511-25.

4.   Stöber W, Fink A, Bohn E. Controlled growth of monodisperse silica spheres in the micron size range. Journal of Colloid and Interface Science 1968;26(1):62-69.

5.   Bogush GH, Tracy MA, Zukoski Iv CF. Preparation of monodisperse silica particles: Control of size and mass fraction. Journal of Non-Crystalline Solids 1988;104(1):95-106.

6.   Chrusciel J, Slusarski L. Synthesis of nanosilica by the sol-gel metod and its activity toward polymers Materials Science & Engineering C-Materials for Biological Applications 2003;21(4):461-69

7.   Chen S-L, Dong P, Yang G-H, Yang J-J. Kinetics of Formation of Monodisperse Colloidal Silica Particles through the Hydrolysis and Condensation of Tetraethylorthosilicate. Industrial & Engineering Chemistry Research 1996;35(12):4487-93.

8.   Jafarzadeh M, Rahman IA, Sipaut CS. Synthesis of silica nanoparticles by modified sol–gel process: the effect of mixing modes of the reactants and drying techniques. Journal of Sol-Gel Science and Technology 2009;50(3):328-36.

9.   EP P. silane coupling agents. 2 ed. New York: Plenum Press; 1991.

10. Miller JD, Ishida H. Quantitative monomolecular coverage of inorganic particulates by methacryl-functional silanes. Surface Science 1984;148(2):601-22.

11. B A. Silane coupling agent chemistry. Pennsylvania:Petrarch Systems Catalorue 1987:59.

12. Posthumus W, Magusin PCMM, Brokken-Zijp JCM, Tinnemans AHA, van der Linde R. Surface modification of oxidic nanoparticles using 3-methacryloxypropyltrimethoxysilane. Journal of Colloid and Interface Science 2004;269(1):109-16.

13. Söderholm K-JM, Shang S-W. Molecular Orientation of Silane at the Surface of Colloidal Silica. Journal of Dental Research 1993;72(6):1050-54.

14. Pires-de-Souza FdCP, Panzeri H, Vieira MA, Garcia LdFR, Consani S. Impact and fracture resistance of an experimental acrylic polymer with elastomer in different proportions. Materials Research 2009;12:415-18.

15. Vojdani M, Giti R. Polyamide as a Denture Base Material: A Literature Review. Journal of Dentistry 2015;16(1 Suppl):1-9.

16. Alhareb AO, Akil HM, Ahmad ZA. Impact strength, fracture toughness and hardness improvement of PMMA denture base through addition of nitrile rubber/ceramic fillers. The Saudi Journal for Dental Research 2016:1-9.

17. Chaijareenont P, Takahashi H, Nishiyama N, Arksornnukit M. Effect of different amounts of 3-methacryloxypropyltrimethoxysilane on the flexural properties and wear resistance of alumina reinforced PMMA. Dent Mater J 2012;31(4):623-8.

18. Gupta R, Kennel E, Kim K-J. Overview of Challenges and Opportunities. Polymer Nanocomposites Handbook: CRC Press; 2009.

19.   Kim K- J, White J. Nanoparticle Dispersion and Reinforcement by Surface Modification with Additives for Rubber Compounds. Polymer Nanocomposites Handbook: CRC Press; 2009.

20.   Clogston JD, Patri AK. Zeta potential measurement. Methods Mol Biol 2010;697:63-70.

21.   Iler RK. The chemistry of silica; 1979.

22.   Kim K- J, White J. Dispersion of Agglomerated Nanoparticles in Rubber Processing. Polymer Nanocomposites Handbook: CRC Press; 2009.

23.   Shokoohi S, Arefazar A, Khosrokhavar R. Silane Coupling Agents in Polymer-based Reinforced Composites: A Review. Journal of Reinforced Plastics and Composites 2008;27(5):473-85.

24.   Arksornnukit M, Takahashi H, Nishiyama N. Effects of silane coupling agent amount on mechanical properties and hydrolytic durability of composite resin after hot water storage. Dent Mater J 2004;23(1):31-6.

25.   Karabela MM, Sideridou ID. Effect of the structure of silane coupling agent on sorption characteristics of solvents by dental resin-nanocomposites. Dent Mater 2008;24(12):1631-9.

26.   Wang Y, Li Y, Zhang R, Huang L, He W. Synthesis and characterization of nanosilica/polyacrylate composite latex. Polymer Composites 2006;27(3):282-88.

27.   Joseph HK.   Characterization of Polymer Nanomaterials.   Polymer Nanocomposites: Processing, Characterization, and Applications: McGraw Hill Professional, Access Engineering; 2006.

28.   Shekunov BY CP TH, Chow AL. Particle Size Analysis in Pharmaceutics: Principles, Methods and Applications. Pharmaceutical Research 2006;24:203-26.

29.   Sing KSW, Everett DH, Haul RAW, et al. Reporting physisorption data for gas/solid systems with special reference to the determination of surface area and

porosity (Recommendations 1984). Pure and Applied Chemistry 1985;57(4):603-19.

30.   ISO 9277:2010. Determination of the specific surface area of solids by gas adsorption. BET method. 2nd ed Intenational Organization Standardization, 2010.

31.   Mauger M DA, Halary J. Synthesis and physico-chemical characterization of networks based on methacryloxypropyl-grafted nano-silica and methyl methacrylate. Polym. Int 2004;53:378-85.

32.   Elimelech M, Chen WH, Waypa JJ. Measuring the zeta (electrokinetic) potential of reverse osmosis membranes by a streaming potential analyzer. Desalination 1994;95(3):269-86.

33.   Kirsten WJ. CHAPTER 9 - AUTOMATIC SIMULTANEOUS DETERMINATION OF CARBON, HYDROGEN, AND NITROGEN*. Organic Elemental Analysis: Academic Press; 1983:43-51.

34.   ISO 20795-1:2013 I. Dentistry -- Base polymers -- Part 1: Denture base polymers, 2nd ed Intenational Organization Standardization, Geneva 2013.

35.   Nishiyama N, Shick R, Ishida H. Adsorption behavior of a silane coupling agent on colloidal silica studied by gel permeation chromatography. Journal of Colloid and Interface Science 1991;143(1):146-56.

36.   Vrancken KC, Van Der Voort P, Possemiers K, Vansant EF. Surface and Structural Properties of Silica Gel in the Modification with γ-Aminopropyltriethoxysilane. Journal of Colloid and Interface Science 1995;174(1):86-91.

37.   Young GJ. Interaction of water vapor with silica surfaces. Journal of Colloid Science 1958;13(1):67-85.

38.   Htang A, Ohsawa M, Matsumoto H. Fatigue resistance of composite restorations: Effect of filler content. Dental Materials 1995;11(1):7-13.

39.   Islam MS, Masoodi R, Rostami H. The Effect of Nanoparticles Percentage on Mechanical Behavior of Silica-Epoxy Nanocomposites. Journal of Nanoscience 2013;2013:10.

40.   Becker WT LS. Fracture appearance and mechanisms of deformation and fracture. ASM International 2002:35-41.

41.   Zhang X-Y, Zhang X-J, Huang Z-L, Zhu B-S, Chen R-R. Hybrid effects of zirconia nanoparticles with aluminum borate whiskers on mechanical properties of denture base resin PMMA. Dental Materials Journal 2014;33(1):141-46.

42.   Khashayar G, Bain PA, Salari S, et al. Perceptibility and acceptability thresholds for colour differences in dentistry. Journal of Dentistry 2014;42(6):637-44.

43.   Johnston WM, Kao EC. Assessment of Appearance Match by Visual Observation and Clinical Colorimetry. Journal of Dental Research 1989;68(5):819-22.

44.   Kuehni RG MR. An experiment in visual scaling of small color differences. Color Res 1979;4:83-91.

APPENDIX

VITA

Mr. Pornpot Jiangkongkho was born on April 19th, 1981 in Uttaradit province, Thailand. He graduated the degree of Doctor of Dental surgery with Honors from Faculty of Dentistry, Naresuan University in 2005. He started working as the lecturer in Prosthodontics department, Faculty of Dentistry, Naresuan University in 2005. He attended the Master of Science Program in Prosthodontics, Faculty of Dentistry, Chulalongkorn university and graduated in 2012. After that, he attended the Doctor of Philosophy Program in Prosthodontics, Faculty of Dentistry, Chulalongkorn university.